SCIENCE CHINA
Chemistry

•REVIEWS•

May 2023 Vol.66 No.5: 1261–1287
https://doi.org/10.1007/s11426-022-1515-5

Trisubstituted alkenes featuring aryl groups: stereoselective synthetic strategies and applications

Meng-Yao Li[1,2†], Shuyang Zhai[1†], Xiao-Mei Nong[1,3], Ao Gu[1], Jiatong Li[1], Guo-Qiang Lin[2*] & Yingbin Liu[1*]

[1]*Shanghai Cancer Institute, Renji Hospital Affiliated to Shanghai Jiao Tong University School of Medicine, Shanghai 200127, China;*
[2]*Shanghai Institute of Organic Chemistry, Chinese Academy of Sciences, Shanghai 200032, China;*
[3]*School of Basic Medicine and Clinical Pharmacy, China Pharmaceutical University, Nanjing 211198, China*

Received November 21, 2022; accepted January 17, 2023; published online April 17, 2023

In recent years, the synthesis and application of alkenes have attracted increased attention. Triphenylethenes (TriPEs) have lower molecular torsion than tetraphenylethenes (TPEs), which helps to balance the degree of conjugation and the aggregation-induced emission (AIE) effect. The geometry of double bonds has a significant impact on luminescence. Therefore, it is essential to provide a comprehensive summary of the stereoselective synthetic strategies for trisubstituted alkenes. In this review, common strategies for the stereoselective synthesis of alkenes are described, with an emphasis on the origin of stereoselectivity and the types of substrates. In addition, the AIE properties of TriPE and its applications in optoelectronic devices, stimuli-responsive materials, sensors, and therapies were discussed.

trisubstituted alkenes, stereoselective synthesis, aggregation-induced emission, transition metal catalysis

Citation: Li MY, Zhai S, Nong XM, Gu A, Li J, Lin GQ, Liu Y. Trisubstituted alkenes featuring aryl groups: stereoselective synthetic strategies and applications. *Sci China Chem*, 2023, 66: 1261–1287, https://doi.org/10.1007/s11426-022-1515-5

1 Introduction

Alkenes are an important class of functional molecules that are widely employed in materials, medicines, pesticides, fragrances, and other applications [1]. Furthermore, the alkene double bond is very reactive, capable of reacting with a wide range of electrophilic and nucleophilic compounds. Therefore, the synthesis of alkene has long been of great interest to chemists. Trisubstituted alkenes, particularly triarylsubstituted alkenes, are frequently employed in optoelectronics, chemical sensing, and bioimaging. It is crucial to examine their synthesis methods and applications in more detail.

Because of the universality of alkenyl double bonds, a variety of synthetic methods have been developed, including stoichiometric reactions (such as the Wittig [2] and Julia [3] reactions) and transition metal-catalyzed reactions (like the olefin metathesis [4] and Heck reactions [5]). Although these methods offer a variety of practical ways to synthesize alkenes, the stereoselective synthesis of trisubstituted alkenes, particularly aryl groups containing trisubstituted alkenes, remains a long-standing challenge in organic chemistry due to the small energy differences between their *E* and *Z* isomers (in comparison to 1,2-disubstituted alkenes). The stereoselective synthesis of trisubstituted alkenes is extremely difficult due to the isomerization of double bonds when exposed to light, heat, bases, or catalysts [6,7]. Therefore, it is necessary to examine and summarize the stereoselective synthesis of trisubstituted alkenes.

The numerous potential applications of luminescent materials have attracted a lot of attention. However, owing to

†These authors contributed equally to this work.
*Corresponding authors (email: lingq@sioc.ac.cn; laoniulyb@shsmu.edu.cn)

intermolecular π-π stacking interactions between fluorogens, many fluorescent compounds that display strong emission in diluted fluids experience aggregation-caused quenching (ACQ) in the solid state, severely limiting their applications [8]. Fortunately, Tang *et al*. [9] revealed an interesting and opposing phenomenon known as aggregation-induced emission (AIE) in 2001. It explains a photophysical phenomenon involving luminescent materials that are non-emitting in their molecular state but emit strongly in their aggregate state. Numerous luminogens with favorable AIE features have been described over the last two decades [10–13]. This phenomenon was described using the idea of restricted intramolecular motion (RIM), which includes both restricted intramolecular vibration (RIV) and restricted intramolecular rotation (RIR) [14–16].

Tetraphenylethylenes (TPEs), a well-known AIE luminogen, are typical AIEgens having a unique AIE effect and a clear and simple molecular scaffold. Several reviews [17–19] have focused on the properties of such skeletons. In addition, Zhao *et al*. [20] highlighted the various common methodologies for the stereoselective synthesis of TPEs, such as McMurry coupling, Rathore's procedures, Suzuki coupling, and multi-component coupling. In contrast to TPEs, triphenylethylenes (TriPEs) are gradually raising issues due to their lower degree of molecular torsion and variable degree of conjugation. Despite the widespread use of TriPEs, a systematic assessment of their synthesis and uses is still required. Therefore, this review focuses on the stereoselective synthetic strategies and applications of trisubstituted alkene-based AIEgens.

In this review, the stereoselectivity of double bonds with regard to synthesis is explored. Several strategies for the stereoselective synthesis of trisubstituted alkenes have been described, including (1) coupling with disubstituted alkenes; (2) insertion of alkynes; (3) isomerization of terminal alkenes; and (4) cleavage of carbon-fluorine bonds. Several techniques that were inapplicable to aryl groups containing trisubstituted alkenes were excluded, and sporadic examples that included specific skeletons were not shown either. Since *Z*- and *E*-alkenes can be rapidly synthesized *via* stereo-divergent synthesis of trisubstituted alkenes, this section is also thoroughly summarized. This review is concerned with the most recent applications of TriPEs derivatives in optoelectronic devices, stimuli-responsive materials, sensors, therapies, and other fields.

2 Stereo-synthesis of trisubstituted alkenes

Depending on the substrates, two primary methods can be utilized in the stereoselective synthesis of alkenes. One way to synthesize alkenes is to use substrates not containing unsaturated bonds (such as haloalkanes, alcohols, or quaternary ammonium salts), which can be converted to alkenes *via* the *β*-elimination process. As this strategy has already been extensively examined, it will not be discussed further in this review.

Using substrates with unsaturated bonds is an alternative method of alkene synthesis. Trisubstituted alkenes can be produced from a variety of starting materials including aldehydes, ketones, alkenes, and alkynes.

Besides reacting with Ylides reagents (through Wittig, Horner-Wadsworth-Emmons, Peterson, and Julia olefination), the carbonyl group can also react with active methylene compounds (by Knoevenagel condensation) to yield the corresponding alkenes. The Ylides salt controls stereochemistry in Wittig reactions. Additionally, in Knoevenagel reactions, the steric effect regulates the geometry of the product and favorably produces thermodynamically stable alkenes. Since these two procedures for the synthesis of multi-aryl alkenes offer only weak stereoselectivity, we will not explore them in detail here.

Alkynes are a type of highly unsaturated compounds that produce trisubstituted alkenes through the hydrocarbonation process. Due to the difficulty of applying this type of reaction to the synthesis of multiaryl alkenes, alkyne-alkyne and alkyne-alkene dimerization were ruled out.

Alkenes are another type of effective substrate that involves three different types of reactions. The first is the synthesis of higher alkenes from lower alkenes, which includes Heck coupling, radical addition, and activation of alkenyl C−H bonds. The second procedure involves the isomerization of an alkene. The final type is the derivatization of alkene synthons. The aforementioned three strategies will be discussed extensively because they offer numerous options for controlling double-bond stereoselectivity.

It is worth noting that alkene synthons, as previously discussed, include alkenyl bromides, alkenyl borons, and alkenyl silicides. When these compounds were used as substrates, the synthesis of stereo-defined trisubstituted alkenes frequently necessitated the use of a single geometry of substrates, which are often more difficult to get. Additionally, stereo-convergent reactions were rather uncommon. *Z*/*E* isomerization also occurred during the reaction, which made it difficult to get pure products. In addition, the mechanisms by which these reactions occur have been investigated extensively. The above-mentioned three types of substrates will not be discussed in light of the aforementioned three factors. Because of their unique characteristics, alkenyl fluoride compounds have attracted significant attention in recent years. Alkenes are more susceptible to nucleophilic attack owing to the electron-withdrawing properties of fluorine atom. The olefin derivatization process is then possible as a result of the *β*-F elimination. In addition, radical addition and C−F bond activation are viable methods for implementing this strategy. As a re-

sult, for the synthesis of trisubstituted alkenes from alkene synthons, only processes using fluoroalkenes as substrates are discussed.

2.1 Coupling reaction involving disubstituted alkenes

Disubstituted alkenes are suitable synthons for trisubstituted alkene synthesis. Effective substrates include both 1,1-disubstituted and 1,2-disubstituted alkenes. Based on the reaction mechanism, it can be divided into three categories: (1) Heck reaction; (2) activation of alkenyl C−H bonds; and (3) radical reaction. These three strategies are discussed in greater detail below.

2.1.1 Mizoroki-Heck reaction

Heck reaction with 1,2-disubstituted alkenes. Internal alkenes often exhibit weak stereoselectivity and low reactivity, even though monosubstituted alkenes are excellent substrates for Heck reactions that produce *trans*-alkene products. A *trans*-internal alkene **1** should produce an *E*-product **2** based on the stereoselectivity of migratory insertion and *β*-H elimination, whereas a *cis*-one **3** can produce a *Z*-product **4** (Scheme 1). However, the Heck reaction with internal alkenes often produced a mixture of *E*- and *Z*-products even when the substrate was a single geometrical isomer. It has been hypothesized that developing a suitable catalytic system to avoid alkene isomerization will considerably increase the stereoselectivity of the Heck reaction with an internal alkene, as the Pd catalyst frequently promotes the isomerization of *cis*-internal alkenes into *trans*-ones.

In the current investigation, three major issues were addressed. (1) How to enhance reactivity; (2) how to improve regioselectivity; (3) how to increase stereoselectivity. Sheppard and Nishikata *et al*. [21] reviewed the Mizoroki-Heck reaction involving internal olefins in 2020. Therefore, the purpose of this section is not to examine specific examples, and a variety of approaches to the aforementioned challenges are also presented.

Due to the weak stereoselectivity of alkyl halides, the Heck arylation reaction has been emphasized. Along with aryl halides **5**, other suitable reagents for this reaction include aryl diazonium salt **6**, arylboron **7**, and aryl-silicon **8**. Alkenes with an electron-withdrawing group (EWG), a directing group (DG), an alkyl-aryl alkene, and an 1,2-diaryl substituted alkene are the four primary types of internal alkene substrates that can effectively participate in this reaction (Scheme 2). The EWG can effectively activate alkenes to initiate the Heck reaction sequence. The regioselectivity was controlled by the inductive effect of the EWG, and the aryl group was usually added to the *β*-site of the EWG. Similarly, DG can activate alkene substrates caused by heteroatom chelation to the metal center, and it can also modulate regioselectivity to provide *β*-site selectivity by forming stable cyclometalated species. For aryl-alkyl substituted alkenes, selecting a suitable catalytic system and controlling regioselectivity through steric effects can make these substrates effective. There is currently no efficient way for regulating the regioselectivity of 1,2-diarylalkene substrates due to their relatively close steric hindrance.

Some issues remain unresolved despite significant efforts. The existence of convergent Heck reactions using (*E*,*Z*)-mixed alkenes is currently unknown. When (*E*,*Z*)-mixed substrates **9** were utilized in the reaction, (*E*,*Z*)-mixed products **11** with the same (*E*,*Z*) ratios as the starting materials were formed (Scheme 3) [22]. Moreover, whereas *trans*-1,2-disubstituted alkenes were used to synthesize stereo-defined trisubstituted alkenes using a variety of strategies, *cis*-1,2-disubstituted alkenes were rarely used as substrates. One possible explanation is that *cis*-alkenes are easily isomerized, resulting in decreased stereoselectivity. On the other hand,

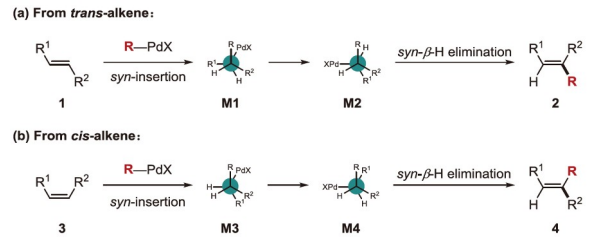

Scheme 1 Mizoroki-Heck reactions involving internal alkenes (color online).

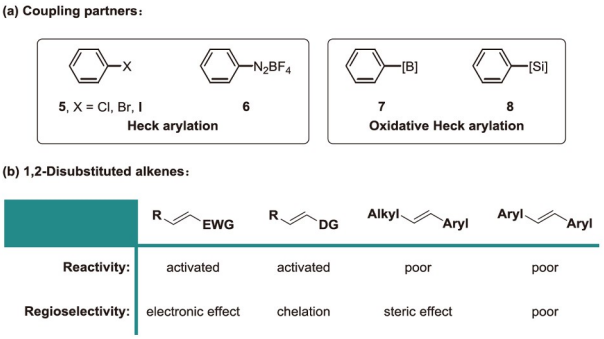

Scheme 2 The type of substrates in Heck reactions (color online).

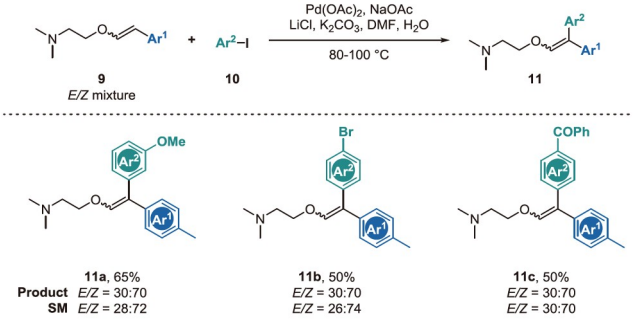

Scheme 3 Heck reactions using (*E*,*Z*)-mixed substrates (color online).

the *cis*-alkenes may have exhibited poor reactivity.

Although the majority of examples employed *trans*-alkene substrates to produce *Z*-selective trisubstituted alkenes, several references displayed the opposite stereoselectivity. Park *et al*. [23] unexpectedly found an oxidative Heck reaction involving *cis*-alkenylamide **12** that produces *Z*-alkenes **13** (Scheme 4). Unfortunately, the authors were unable to explain this unique stereoselectivity.

Chou *et al*. [24] described a palladium-catalyzed Heck arylation reaction employing 1,2-disubstituted alkenes in the presence of carboxylate in which the free carboxylic acid was used as the DG to control the regio- and stereoselectivities (Scheme 5). When utilized as the substrate, *trans*-*β*-cyclohexadienyl methyl acrylate **14** displayed an unexpected stereoselectivity. This stereoselectivity can be explained by an *anti*-*β*-hydride elimination process, which occurs when carboxyl and ester groups are chelated with a palladium center (**M5**), resulting in a stable palladacycle intermediate that limits *syn*-*β*-hydride elimination. The stereoselectivity was reversed when the ester group was substituted with an aryl group (**17**) because the rotation of the carbon-carbon bond might produce a *cis*-*β*-H eliminated conformation in the absence of ester coordination. Ester groups were ineffective replacements for carboxyl-directing groups in commencing this reaction. Notably, 1,2-diaryl substituted alkenes **19a** can also give rise to highly regio- and stereoselective triaryl alkenes **20a**.

Heck reaction with 1,1-disubstituted alkenes. Using 1,1-disubstituted alkenes as substrates provides an alternative method for the synthesis of trisubstituted alkenes (Scheme 6). However, stereoselective synthesis was still challenging, even though this method did not require regioselectivity. Steric effects dominate stereoselectivity in this process, which primarily employs four types of substrates. When 1,1-disubstituted alkenes containing electron-withdrawing substituents are used, an *E*-selective product can be observed. Consequently, alkyl-substituted substrates provided the reaction with significantly higher stereoselectivity than aryl-substituted substrates. In addition, aryl-alkyl substituted alkenes exhibited *E*-selectivity, whereas diaryl alkenes formed only an (*E*,*Z*)-mixture of trisubstituted alkenes.

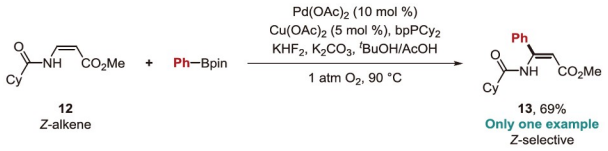

Scheme 4 Oxidative Heck reaction related to *cis*-alkenylamide (color online).

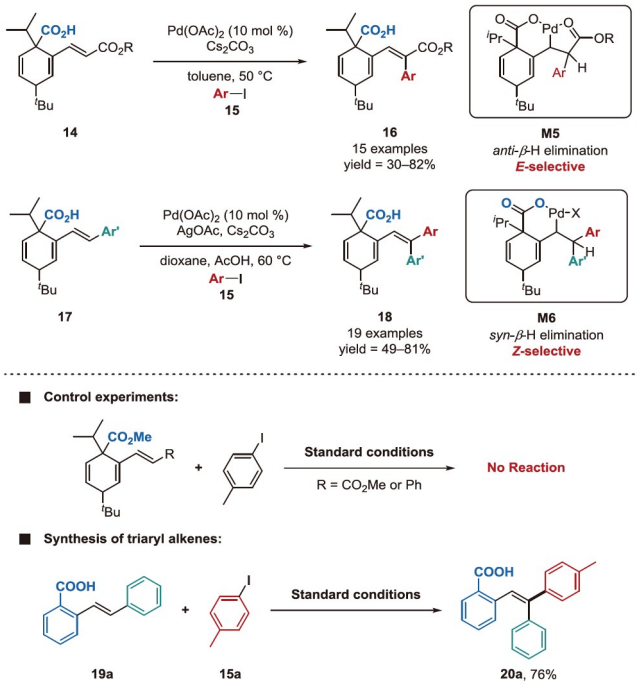

Scheme 5 Carboxylate-assisted palladium-catalyzed Heck reaction with significant stereo- and regioselectivity (color online).

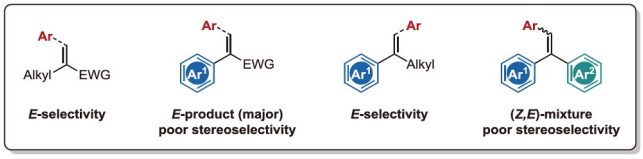

Scheme 6 Heck reaction with 1,1-disubstituted alkenes (color online).

2.1.2 *Alkenyl C−H bond activation*

Directed C−H bond activation of arenes is well-established; however, efficient directed C−H bond activation on vinylic substrates has received less attention. This is probably due to the increased versatility and reactivity of alkenes. However, a lot of effort needs to be done before stereoselective C−H bond activation of vinylic substrates may be utilized as essential intermediates in new cross-coupling reactions that yield valuable, highly substituted alkenes. Several examples of stereoselective alkenyl C−H bond activation/arylation (and alkylation) of 1,1- or 1,2-disubstituted alkenes are discussed in this review. Both the DG and the traceless directing group (TDG) strategies can be used in this process. Activation of the alkenyl C−H bond aided by the chelation effect typically resulted in *cis*-arylation/alkylation of the DG, but isomerization promoted by transition metals became detrimental factors.

Chelation-assisted alkenyl C−H bond arylation. As an effective directing group, pyridyl could provide excellent stereoselectivity for the arylation of the alkenyl C−H bond. Inoue *et al*. [25] used ruthenium catalysis to arylate alkenylpyridines **21** with aryl bromides **22** (Scheme 7). The 1,2-disubstituted substrate was converted into the less stable *β*-arylated-(*Z*)-2-alkenylpyridines **23** as a result of the *cis*-C−H bond activation (**M7**), and the geometry of the products

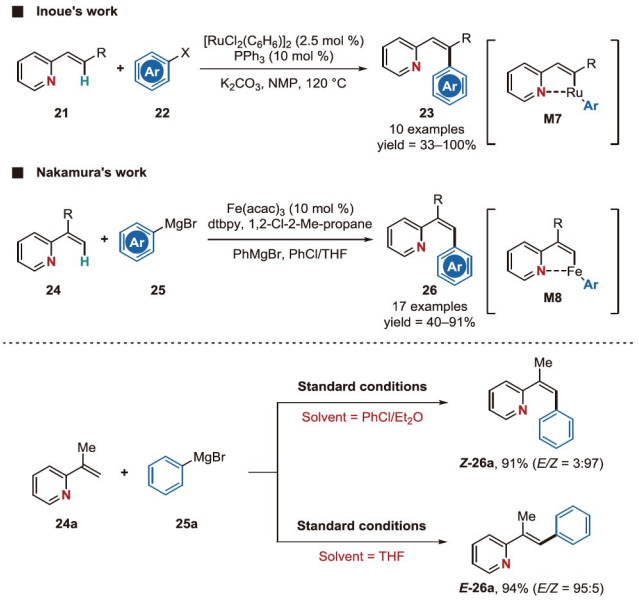

Scheme 7 Pyridyl-assisted alkenyl C−H bond arylation (color online).

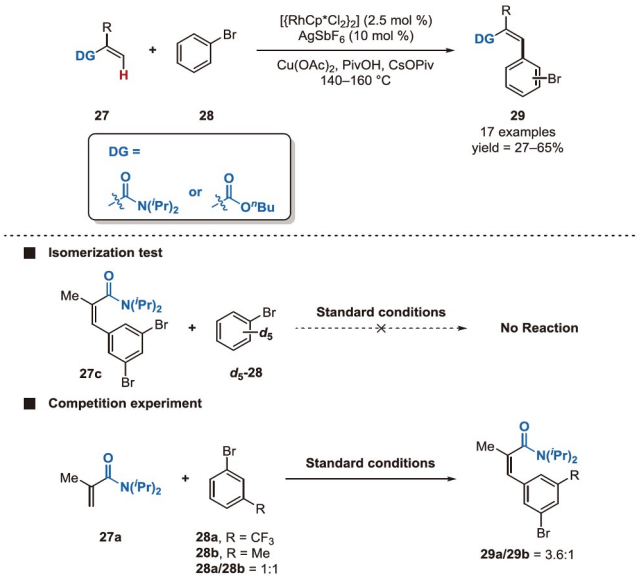

Scheme 8 An amide group assisted arylation of an alkenyl C−H bond (color online).

differs noticeably from that of the aforementioned Mizoroki-Heck reaction. Nakamura *et al*. [26] found that iron-catalyzed arylation of 1,1-disubstituted alkenes **24** could be accomplished with aryl magnesium bromides **25** as the transmetalation reagent. There is a quick and efficient way to synthesize 1,2-diaryl trisubstituted alkenes **26**. This study demonstrated that changing the solvent can affect the stereoselectivity of the product. The authors hypothesized that the aromatic solvent acted as a ligand for the low-valent iron species, preventing it from interacting with the alkene product and, hence, the *E*/*Z* isomerization.

In addition to the pyridine ring, the amide and ester groups have been demonstrated to be effective directing groups for the stereoselective activation of the C−H bond in alkenes. To cross-couple bromoarenes **28** and vinylic substrates **27** with DGs, Glorius *et al*. [27] established a dehydrogenative Rh^{III}-catalyzed reaction (Scheme 8). In this study, *Z*-selectivity was identified in the ester- and amide-directing groups. Further processing of the stereo-defined product did not result in the isomerization of the double bond or any significant H/D scrambling between the solvent and the olefinic proton, indicating that vinylic C−H bond activation can only occur in the *Z*-position relative to the directing group. According to some evidence, the subsequent arylation was caused by aryl C−H bond activation rather than electrophilic substitution.

Chelation-assisted alkenyl C−H bond alkylation. Alkenes are efficient alkylating agents for capturing intermediates of the alkenyl metal (Scheme 9). First, the coordination of the DG resulted in the production of the alkenyl cyclometalated species **M9** *via* the selective activation of alkenyl C–H bonds. Subsequently, $C(sp^2)$–$C(sp^3)$ bonds were formed through the migratory insertion of olefins. Finally, alkenes are alkylated through protonation process.

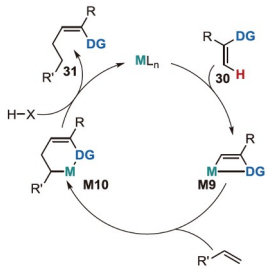

Scheme 9 Chelation-assisted alkenyl C−H bond alkylation (color online).

This method is capable of rapidly synthesizing stereo-defined trisubstituted alkenes, although it has numerous limitations. As alkylation reagents, electron-deficient alkenes were frequently required for effective migratory insertion. Ketone groups were shown to be more suitable than ester groups for avoiding *β*-H elimination competition. Feng and Loh *et al*. [28] used the weakly coordinating directing group *N*-tosyl amide and acryloylsilanes as alkylation reagents to accomplish the Rh-catalyzed alkylation of the alkenyl C−H bond. Furthermore, Zhong *et al*. [29] described a cobalt-catalyzed alkenyl alkylation using *α*,*β*-unsaturated ketones **36** as substrates (Scheme 10).

Shibata *et al*. [30] used *α*,*β*-unsaturated ester substrates **39** to produce the associated conjugate adducts **40** *via* iridium catalysis process. When (*S*)-Tol-BINAP was used as a ligand, internal alkenes can efficiently act as alkylation reagents in this reaction to produce excellent *ee* (Scheme 11). The authors demonstrated their proposed mechanism for the current cross-coupling of two electron-deficient alkenes,

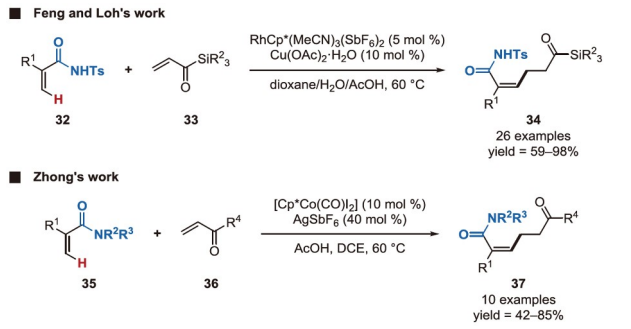

Scheme 10 Amide group-mediated alkylation of an alkenyl C−H bond (color online).

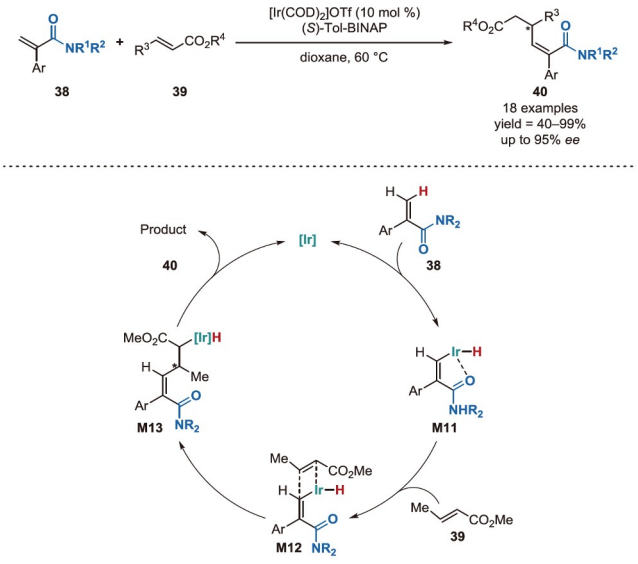

Scheme 11 Cross-coupling between two electron-deficient alkenes through vinylic C–H activation (color online).

which requires the activation of the vinylic C−H bond. The regioselectivity was described using the polarity correlation between the carbon-iridium bond and the C−C double bond.

Alkenyl C−H bond arylation/alkylation facilitated by a traceless directing group. The TDG approach can be used to increase the universality of substrates for alkene synthesis (Scheme 12). The aryl-to-vinyl 1,4-metal migration reaction provides a new approach for the stereoselective synthesis of triarylethylenes and 1,1-diaryl trisubstituted alkenes. The vinyl C−H bond is activated in this mechanism through the formation of metallacycle species and subsequent selective protonation reactions. The stereoselectivity of the products was regulated by the metallacycle species, and the stereodivergent synthesis of tri-substituted alkenes can be achieved by changing the position of the TDG. Halogen atoms and boric acid groups are also effective TDG for commencing the formation of this sequence. Feng and Lin *et al*. [31], for instance, used this method to synthesize stereo-defined triarylsubstituted alkenes **43** by employing aryl borate esters **42** as transmetalation reagents. In addition, the required al-

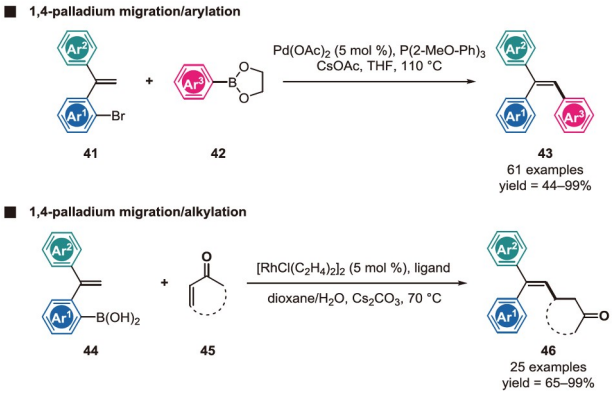

Scheme 12 Alkenyl C−H bond arylation/alkylation facilitated by TDGs (color online).

kylation products were successfully produced by capturing the rhodium migration process through the insertion of alkenes during Rh-migration [32]. There is no need to review this type of reaction again because it was thoroughly discussed in our previous review [33].

2.1.3 Radical-mediated functionalization of alkenes

Trisubstituted alkenes can also be synthesized using a radical addition/elimination reaction. Precursors of the carbon radical, such as bromides, boronic acids, alcohols, and sulfoxide compounds, can be utilized to initiate radical addition sequences. Following deprotonation or the departure of the leaving group (LG), the reaction can be terminated and the C−C double bond can be reformed. Alternatively, a visible light catalytic system can also be used in place of Fe, Ti, and other transition metals in this radical process.

Radical addition/deprotonation reaction. Nishikata *et al*. [34] described an efficient method for the stereoconvergent alkylations of internal alkenes **48** to produce (*E*)-trisubstituted alkenes **49** by using tertiary alkyl bromides **47** as the alkylation reagent (Scheme 13). Various evidences suggested that the stereoselectivity of the alkene was not induced by the *Z*/*E* isomerization of the product. The stereoselectivity of double bonds may be derived from *β*-hydrogen elimination by alkyl iron species. However, this approach is successful for alkylating internal alkenes, whereas it is ineffective for neutral or electron-deficient alkenes.

Zhu *et al*. [35] performed radical addition/deprotonation under photocatalytic conditions utilizing internal alkenes, which remains difficult due to steric congestion on the double bond (Scheme 14). When a *gem*-diaryl alkene **50** was employed as a substrate, tetra-substituted alkene **52** could be produced; however, when an alkylaryl alkene **50′** was utilized, the regioselectivity of deprotonation was changed, producing (*Z*)-trisubstituted alkene **52′**. It could be explained by base-promoted deprotonation, which typically favors a less constrained site. It is worth noting that this method can yield a series of trisubstituted alkenes containing azide

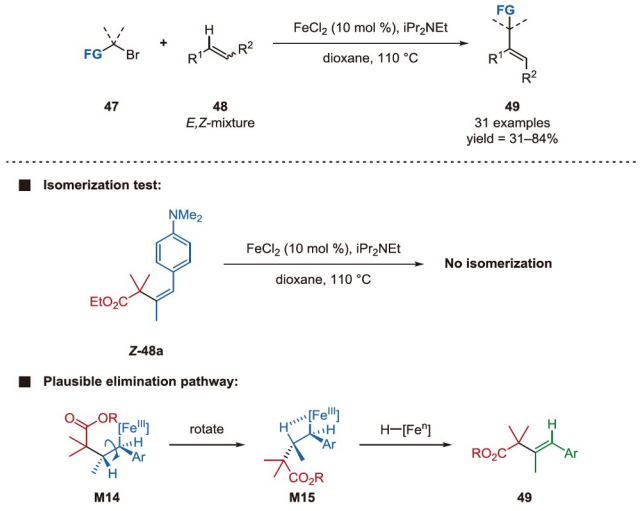

Scheme 13 Stereo-convergent internal alkene alkylations (color online).

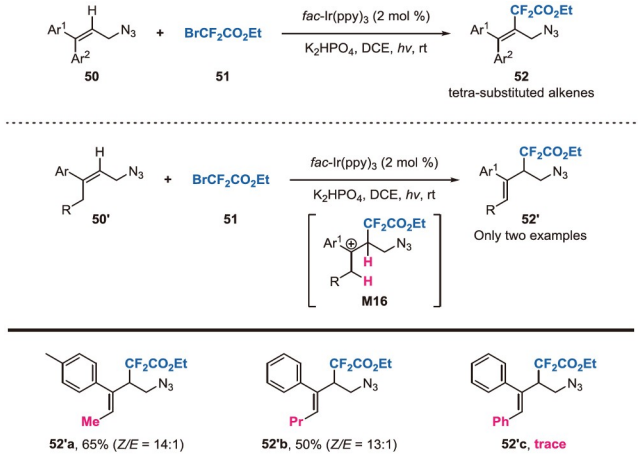

Scheme 14 Light-induced radical addition/deprotonation process (color online).

groups, which can then be easily converted to different types of functional molecules.

In addition to bromides, sulfoxide compounds **54** can also be utilized in the synthesis of trisubstituted alkenes (Scheme 15) [36]. Both 1,1- and 1,2-disubstituted alkenes **53** are effective substrates. Using various sulfoxide compounds, arylation and alkylation processes can be carried out effectively. A series of mechanistic experiments demonstrated that the reaction took place *via* radical addition. The benzyl radical was trapped by the OH radical in the presence of hydrogen peroxide to produce benzyl alcohol, which was then employed in an elimination reaction to yield trisubstituted alkene. The steric effect was responsible for regulating the stereoselectivity of alkenes.

Radical addition/LG departure process. In addition to deprotonation, this protocol can be effectively terminated by the departure of the LG. Baylis-Hillman acetates are an effective substrate for the synthesis of several trisubstituted

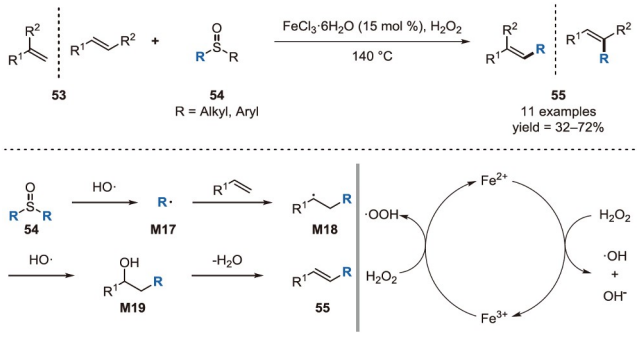

Scheme 15 Fe-catalyzed radical addition/elimination reaction using sulfoxide compounds as substrates (color online).

alkenes.

Singh *et al*. [37] discovered a metal-free procedure for the photoredox synthesis of allylic-trifluoromethylation alkenes **57** using widely available CF_3SO_2Na as the CF_3 source (Scheme 16). The presence of the electron-donating substituent on the aromatic ring exhibits excellent stereoselectivity when compared to the electron-withdrawing groups, indicating that the stereochemistry of the products is probably regulated by the electronic factor.

Suga and Ukaji *et al*. [38] achieved the addition/elimination of 2-carboxy-allyl acetates **59** *via* a radical-ionic process under Ti^{IV}/Mn^0 catalyzed conditions (Scheme 17) using benzyl alcohol **58** as a radical precursor. Trisubstituted alkenes with ester groups **60** can be readily synthesized with an exclusive (*E*)-stereoselectivity. According to the authors, the reaction is triggered by Ti-mediated homolytic C−O bond cleavage and involves the radical addition of alkenes. The source of the stereoselectivity of products was not explained.

Using iridium catalysis, alkyl boronic acid **62** can be employed as a powerful alkyl radical donor to activate this sequence when exposed to visible light (Scheme 18) [39]. The reaction proceeded well with *N*-Boc-protected tetrahydropyrrole-2-borate (**63c**), yielding exclusively the *E*-isomer, possibly due to the steric effect and the stabilizing impact of the nitrogen atom on *ortho* carbon radicals. Despite the fact that the stereoselectivity of this reaction for major substrates is relatively low, it provides a new approach for the rapid synthesis of aryl-substituted alkenes containing trifluoromethyl **63**.

2.2 Stereo- and regioselectivity insertion into alkynes

The insertion of carbon-metal species into alkynes offers an alternative method for obtaining trisubstituted alkenes, using three strategies: (1) internal alkyne hydrocarbonation; (2) transition metal-catalyzed multicomponent reaction of terminal alkynes; and (3) a multistep process comprising carbometalation of terminal alkynes (Scheme 19). Given that the three-component reaction of terminal alkyne primarily involves the formation of functional groups containing al-

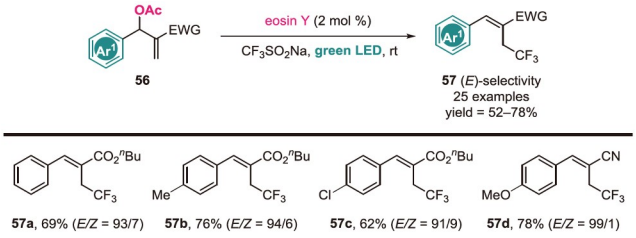

Scheme 16 Radical addition/elimination process initiated by CF_3 radical (color online).

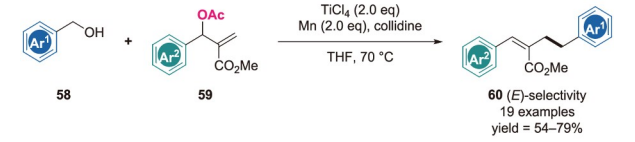

Scheme 17 Ti-mediated addition/elimination reaction (color online).

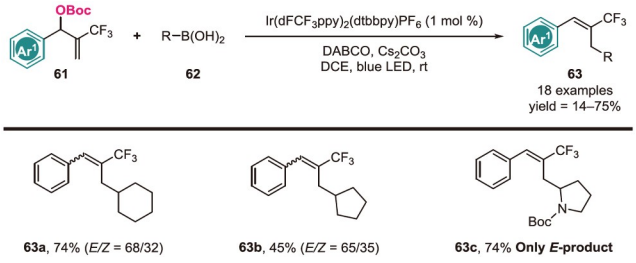

Scheme 18 Radical addition/elimination process initiated by alkyl boronic acid (color online).

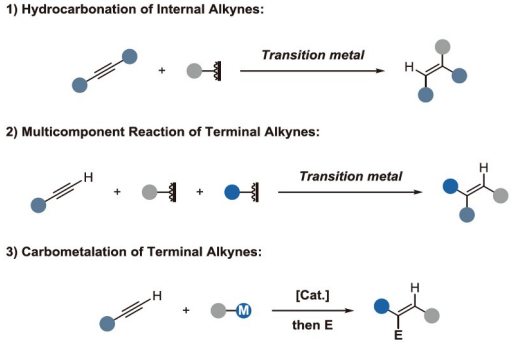

Scheme 19 Insertion of carbon-metal species into alkynes (color online).

kenes, and that the majority of terminal alkyne carbometalation was captured with water as an electrophilic reagent to obtain disubstituted alkenes, these two strategies will not be discussed in detail here. The regio- and stereoselectivity involved in the hydrocarbonation of internal alkynes will be emphasized in this section.

When symmetrical alkynes are used as substrates, the majority of alkyne hydrocarbonation reactions produce *syn*-stereoselectivity, which leads to the synthesis of a single product. Two regioisomeric products were typically produced when unsymmetrically substituted alkyne substrates were used. Different synthesis strategies might be employed depending on the products, as indicated in Scheme 20. The hydrocarbonation of diaryl, dialkyl, and alkylaryl alkyne substrates was discovered to be successful. It is crucial to note that hydroarylation of alkynes is relatively common, whereas hydroalkylation is comparatively uncommon.

There are two typical pathways for controlling regioselectivity for alkylaryl alkyne substrates (Scheme 21). The first is the *syn*-insertion of metal hydrides into alkynes, which results in the formation of an alkenyl metal compound. Following transmetallation (oxidative addition or C−H bond activation) and reductive elimination (Pathway A), an alkene with a single geometry was obtained. The other route involves the incorporation of carbon-metal species into alkynes, followed by protonation to complete the reaction and yield alkenes (Pathway B). Transition metals typically contribute to the aryl side during the migratory insertion process as opposed to the alkyl side. Numerous studies indicate that the coordination of directing groups, steric effects, and electronic effects all contributed significantly to regioselectivity (Scheme 22).

In general, four hydrocarbonation strategies have been applied to alkynes: (1) oxidative addition initiated alkyne insertion; (2) transmetallization initiated alkyne insertion; (3) C−H bond activation initiated alkyne insertion; and (4) electrophilic aromatic substitution of alkyne.

2.2.1 Oxidative addition initiated alkyne insertion

Aryl halides are an excellent electrophile for initiating this insertion process. Typically, aryl iodides were considered appropriate substrates, whereas aryl bromides exhibited restricted reactivity, probably due to the comparatively slow oxidative condition step to alkyne-ligated metal species. In 2018, Jin and Hu *et al.* [40] established the viability of aryl bromides by applying bulky sterically hindered ligands to stabilize the palladium center, thereby giving a simple approach to synthesize 1,2-diaryl trisubstituted alkenes **66** (Scheme 23). The examined substrates had high stereoselectivities, with the majority having *E*/*Z* ratios of 99:1 or above. Although the approach produced comparable products for diarylacetylenes and alkylarylacetylenes, there was a lack of regioselectivity when utilized with unsymmetrical diarylacetylene. This reaction followed an arylpalladium *syn*-insertion process, and alcohol, which served as a reductant, efficiently terminated the reaction *via* *β*-H elimination.

Hull *et al.* [41] showed remarkable regioselectivity of copper-catalyzed 1,1-diaryl trisubstituted alkenes **69** employing alkylarylacetylenes **67** and aryl iodides **68** as substrates, in contrast to palladium-catalyzed alkyne insertion. This was attributable to the high regio- and stereoselectivity of copper hydride insertion (Scheme 24). An alternative investigation indicates that the regioselectivity of the reaction is caused by the electron bias of the alkyne. The in-

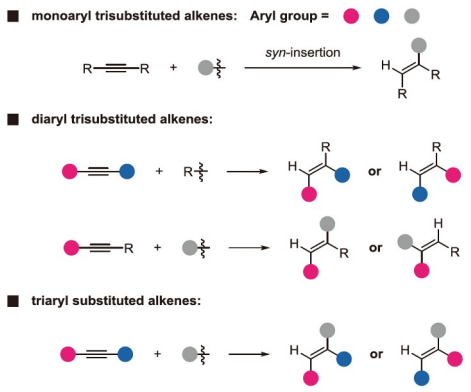

Scheme 20 Common modes of alkyne hydrocarbonation reactions (color online).

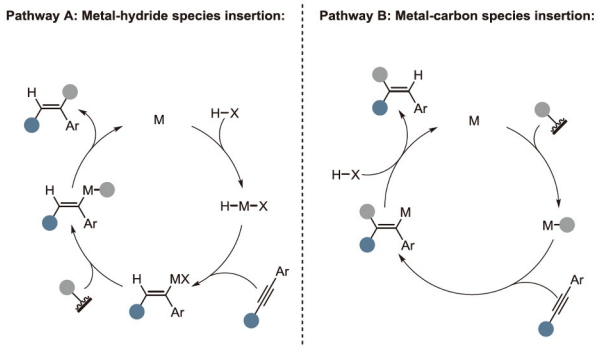

Scheme 21 Two common pathways to control regioselectivity in alkyne insertion (color online).

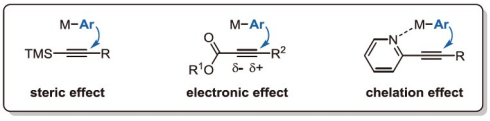

Scheme 22 Factors influencing regioselectivity (color online).

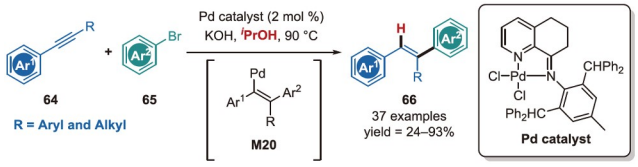

Scheme 23 Pd-catalyzed oxidative addition initiated alkyne insertion (color online).

tramolecular radical clock investigation showed that the reaction was progressing through a two-electron oxidative addition/reductive elimination process after copper hydride species were inserted into alkynes; however, a rapid one-electron oxidative addition approach cannot be ruled out.

2.2.2 *Transmetalization initiated alkyne insertion*

Alkyne insertion could potentially be initiated *via* transmetalization. There are many potential transmetalation reagents, including aryl boric acid, aryl zinc, and aryl diazo

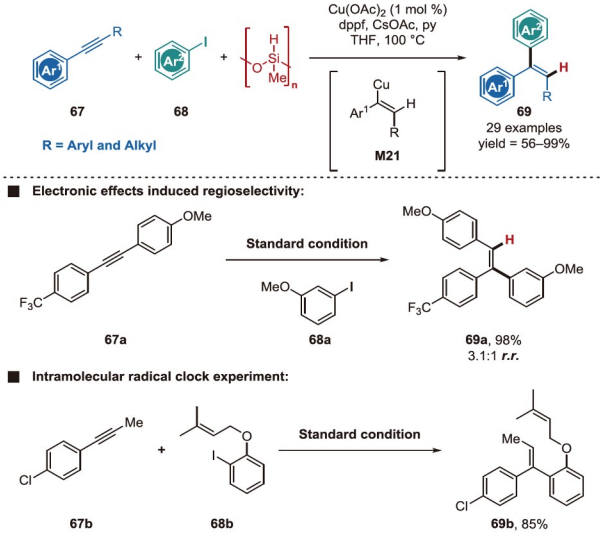

Scheme 24 Cu-catalyzed oxidative addition initiated alkyne insertion (color online).

compounds.

Oh *et al.* [42] first described the palladium-catalyzed hydroarylation of alkynes **70** with organoboronic acids **71** (Scheme 25). The synthesis of 1,1-disubstituted alkenes (**72a** and **72b**) and trisubstituted alkenes (**72c** and **72d**) was achievable using both internal and terminal alkynes. The unsymmetrical alkyne only resulted in a variety of regioisomers of the addition products, whereas the *cis*-addition process yielded a single geometric product. According to the authors, this difference in regioselectivity is attributable to its distinct reaction mechanism, which involves the migratory insertion of alkynes into palladium hydrogen species (as shown in Scheme 21 pathway A).

The directing group strategy was applied to alkyne insertion reactions to address the regioselectivity of this reaction (Scheme 26). Pyridine [43,44], hydroxyl [45], and amino groups [46] are all effective *β*-regioselective directing groups. Moreover, Engle *et al.* [47] utilized a detachable picolinamide (PA) as the directing group (**73**), allowing for modulation of the *β*-selectivity *via* a cleavable bidentate directing group. The substrates dialkyl and alkylaryl alkyne were shown to be compatible.

Although the role of aryl boric acid in catalytic alkyne insertion has been extensively studied, there are still many difficulties with the reaction involving heteroaryl boric acid because the coordination of heteroatoms can lead to catalyst deactivation. Internal alkynes **77** (Scheme 27) have recently been hydro-pyridinated by Dou *et al.* [48] using rhodium as the catalyst. Results were favorable for diaryl, dialkyl, and alkylaryl acetylenes. The pyridylation occurred preferentially at the alkyl side when the arylalkyl alkynes were utilized. Importantly, in contrast to Marinelli's work [46], the amine group is incapable of providing a directing effect, and the only product formed is *α*-regioselective.

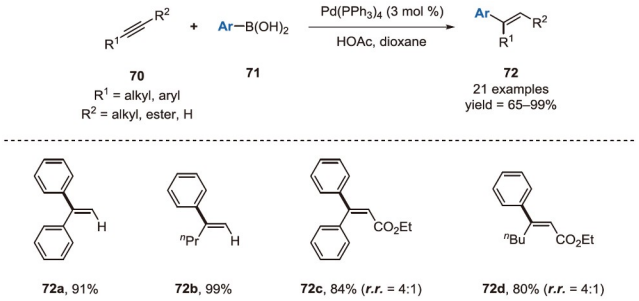

Scheme 25 Pd-catalyzed transmetalization initiated alkyne insertion (color online).

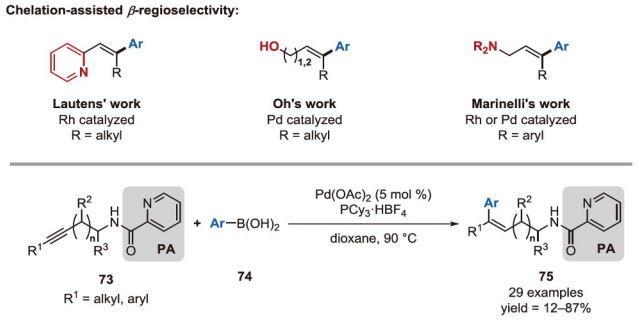

Scheme 26 Directing group-controlled regioselectivity alkyne insertion (color online).

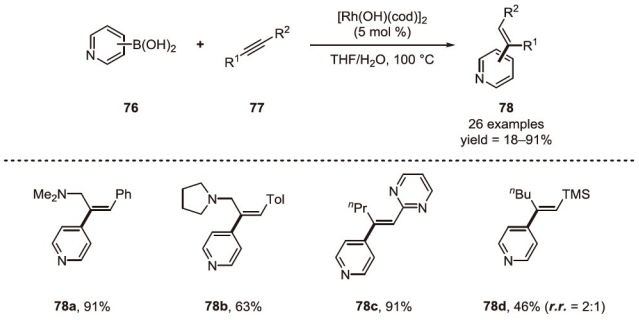

Scheme 27 Alkyne insertion reaction involving pyridyl boric acid.

In addition to aryl boronic acids, the reaction can be carried out with aryldiazonium salts **79**. Cacchi *et al*. [49] reported the hydroarylation of internal alkynes **80** using palladium as the catalyst (Scheme 28). The high yield was achieved by using both electron-rich and electron-deficient aryl diazonium salts. The migratory insertion of the aryl palladium complex resulted in *cis*-addition selectivity. Only diaryl acetylene and aryl ester acetylene were found to be effective substrates. Electronic effects have a minor impact on regioselectivity, and the phenyl group has a greater influence on the direction of addition than the ester groups of the reaction, resulting in α-site selectivity of the ester groups.

Aryl Grignard reagents **83** can be used to initiate such reactions. Hor and Zhao *et al*. [50] carried out the nickel-catalyzed stereoselective arylmagnesiation of internal alkynes **82**, using water as the electrophilic reagent to yield

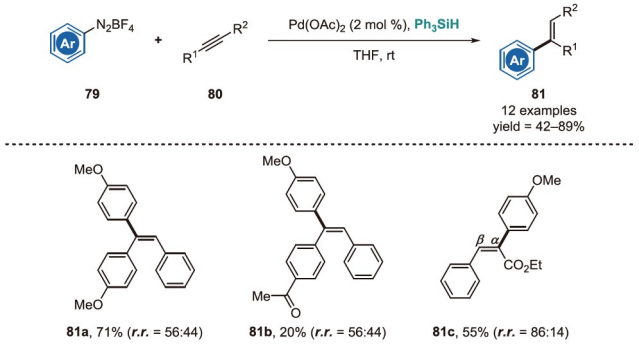

Scheme 28 Alkyne insertion reaction involving aryl diazonium salts (color online).

stereo-defined trisubstituted alkenes **84** (Scheme 29). All reactions produce highly stereoselective products without the use of a directing group. According to the ratios of the resulting *E*/*Z* isomers, all arylmagnesiation reactions proceed *via* a *syn*-addition across the alkyne.

2.2.3 *C−H bond activation initiated alkyne insertion*

DG-assisted cobalt-catalyzed and rhodium-catalyzed aryl C−H bond activation/alkynyl insertion reactions were carried out by Yoshikai *et al*. [51] and Zhou *et al*. [52], respectively. Pyridines (**85**) and benzotriazoles (**88**) are excellent directing groups for initiating C−H bond activation sequences. These two types of reactions demonstrated excellent regio- and stereoselectivity. A series of experiments indicated that these reactions had comparable reaction mechanisms: insertion of C−C triple bonds into metal hydrogen intermediates results in *cis*-stereoselectivity, and subsequent reduction elimination produces stereo-defined trisubstituted alkenes. Deuterium-labeling experiments revealed that C−H bond cleavage or formation was an irreversible reaction step. Interestingly, the regioselectivity of the two aforementioned reactions differs slightly. Unsymmetrical alkynes underwent C−C bond formation at sterically less hindered positions in Yoshikai's work. Zhou's investigation, on the other hand, discovered that when alkylphenyl acetylenes **89** were employed as substrates, C−C bonds tended to form on the aryl-substituted side. The proposed reaction mechanism is shown in Scheme 30.

Although trisubstituted alkenes can be synthesized *via* chelation-assisted C−H bond activation initiated hydrogenarylation of alkynes, this method is still limited by the nature of the *ortho*-directing groups and cannot be used to access *para*- or *meta*-substituted alkenyl arenes. Zhao *et al*. [53] employed carboxyl as TDG to address this issue (Scheme 31). The synthesis of trisubstituted alkenes **93** through the hydroarylation of alkynes using a decarboxylative method resulted in high stereoselectivity for *syn*-hydroarylation. In contrast to prior investigations, aryl groups were more likely to contribute to the alkyl side.

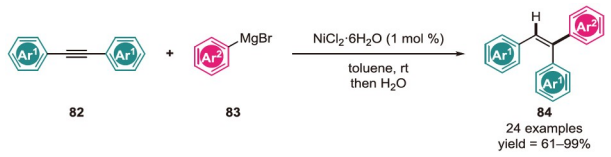

Scheme 29 Alkyne insertion reaction involving aryl Grignard reagents (color online).

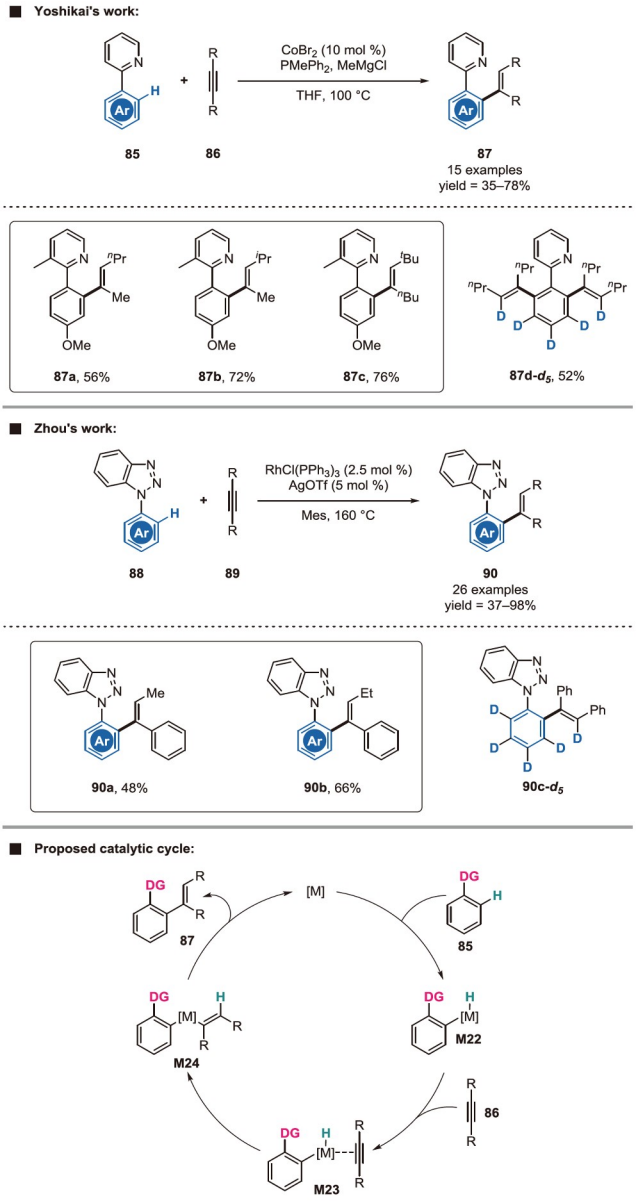

Scheme 30 The activation of C−H bonds initiated the insertion of alkyne (color online).

2.2.4 Electrophilic aromatic substitution initiated alkyne insertion

To obtain the associated hydroarylation products catalyzed by Lewis or Brønsted acids, arenes and alkynes may undergo conventional electrophilic aromatic substitution reactions. There are two restrictions associated with this approach.

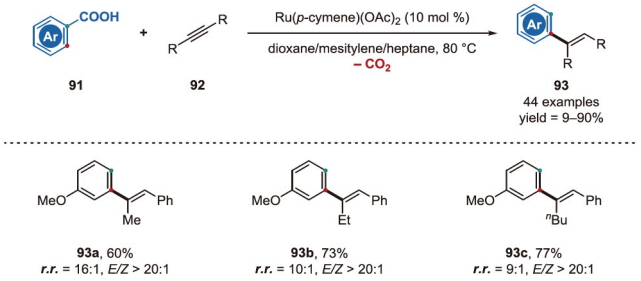

Scheme 31 Hydrogenarylation reactions of alkynes using carboxyl as a traceless directing group (color online).

Initially, the electronic effect of the aromatic ring governed the electrophilic aromatic substitution, and poor regioselectivity was frequently observed. Due to the small energy difference between the *Z*- and *E*-configurations of trisubstituted alkenes, hydroarylation of internal alkynes in the presence of an acid always produces a mixture of *Z*- and *E*-isomers. *Ortho*-electrophilic aromatic substitution was carried out in 2021 by Wang and Li *et al.* [54] employing a phenolic hydroxyl group as the directing group (Scheme 32). Triaryl-substituted alkenes can be produced using a unique *Z*-selective synthesis in the presence of $B(C_6F_5)_3$. When used on unsymmetrical diaryl acetylene, this technique demonstrated great regioselectivity, with only one regioisomer being discovered. According to DFT studies, the electronic effect regulated the regioselectivity of hydroarylation.

2.3 Positional isomerization of terminal alkenes

Positional isomerization of readily accessible terminal alkenes is believed to be a successful strategy for obtaining regio- and stereo-defined alkenes with complete atom economics. The migration of the original C−C double bond, which is driven by a thermodynamically favorable termination step, is one of the distinctive characteristics of this method. Scheme 33 depicts the five basic pathways involved in alkene isomerization according to the mechanisms: (a) metal hydride insertion/elimination mechanism; (b) radical mechanism; (c) carbocation mechanism; (d) mechanism of 1,3-hydrogen shift; and (e) mechanism of oxidative cyclization. Based on the H-transfer process, these mechanisms can be classified into stepwise and concerted pathways. In the following sections, these subjects are examined briefly. Although a systematic summary has been accomplished in prior reviews [55,56], the mechanisms unrelated to the synthesis of aryl groups containing trisubstituted alkenes have not been summarized.

2.3.1 Metal-hydride insertion mechanism

The most frequent method of alkene isomerization is the migratory insertion/*β*-H elimination process of metal hydride species. Positional isomerization of simple *α*-alkyl styrenes

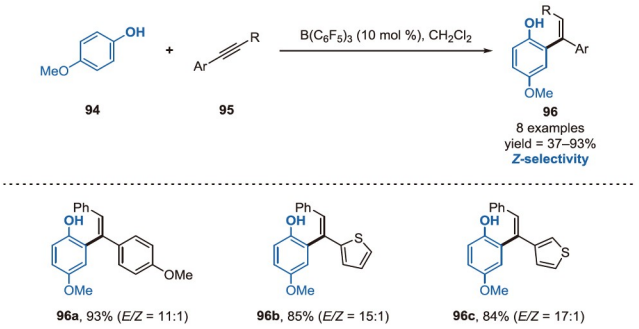

Scheme 32 Alkyne insertion initiated by electrophilic aromatic substitution (color online).

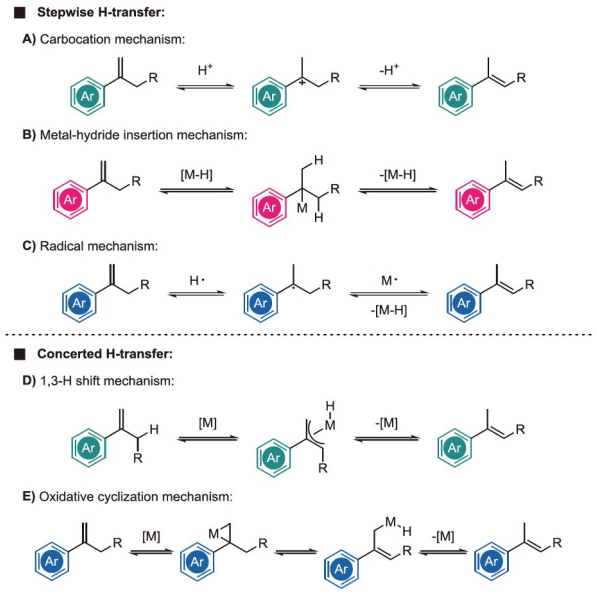

Scheme 33 Mechanisms of alkene isomerization (color online).

to trisubstituted styrenes remains a difficulty due to its poor stereoselectivity and regioselectivity, despite the enormous efforts made over the past few decades to develop effective catalytic methods (such as Ru, Rh, Pd, Ir). There were a few instances of α-alkyl styrenes being stereoselectively isomerized at the start of the 21st century, but until recently, this kind of substrate has not been thoroughly investigated.

Cobalt hydride insertion/elimination pathway. Cobalt hydride species, which can access *E*-trisubstituted alkenes from terminal olefins, were formed *in situ* as a result of the reaction between the divalent cobalt complex and borohydride. Chen and Xia *et al*. [57] published Co-catalyzed isomerization of alkenes using a phosphine-amido-oxazoline (PAO) ligand in 2020 (Scheme 34). High stereoselectivity (*E*/*Z* up to 100/1) and excellent yield were achieved during the conversion of the α-ethyl styrenes **97** to the trisubstituted alkenes **98** that contains monoaryl. The reaction was also applied to internal alkene **99a**, resulting in the formation of (*E*)-β-alkyl styrene **100a** with a high degree of stereo- and benzylic regioselectivity (100/4 ***rr***). Furthermore, an alkene

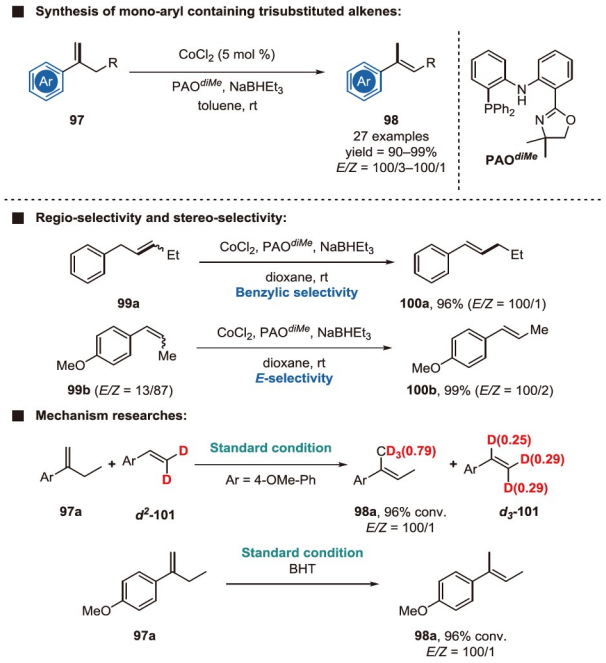

Scheme 34 $CoCl_2$/PAO catalyzed alkene isomerization (color online).

mixture **99b** was easily converted into the *E*-isomer **100b**. Experiments on H/D scrambling and radical capture, respectively, ruled out the possibility of a concerted H-transfer process and suggested that a radical-based HAT mechanistic pathway was incredibly unlikely.

Simultaneously, Lu *et al*. [58] reported a comparable result (Scheme 35). The thiazoline iminopyridine (TIP) ligand was utilized to control the stereoselectivity of the double bond. The isomerization process was conducted at room temperature and in the absence of solvents, making the operation simple. Electron-withdrawing substituents on the phenyl ring reduced the stereoselectivity of this method slightly. The 1,2-disubstituted alkenes **102** are easily isomerized; however, there are no examples of isomerization from internal olefins to trisubstituted olefins in this study.

The steric effect led to the formation of thermodynamically stable *E*-isomers in the preceding two instances. Findlater *et al*. [59] recently revealed a novel method (Scheme 36) for regulating the stereoselectivity of double bonds. The π-π stacking effect and the steric barrier between the catalyst and substrate have demonstrated the capability of controlling stereochemistry. Interestingly, the scope of this isomerization may be expanded to α,β-diaryl groups containing trisubstituted alkenes, which were previously difficult to be produced. Based on the outcomes of the radical trapping and crossover studies, the cobalt hydride insertion/elimination pathway appeared to be the most probable mechanism for the reaction. A slight increase in the ratio of *E* isomer was observed after treating the *E*/*Z* mixture of internal alkenes **106a** (*E*/*Z* = 1/4.4) under standard conditions,

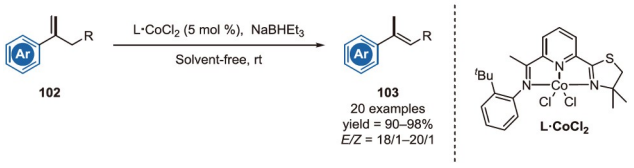

Scheme 35 $CoCl_2$-TIP catalyzed alkene isomerization (color online).

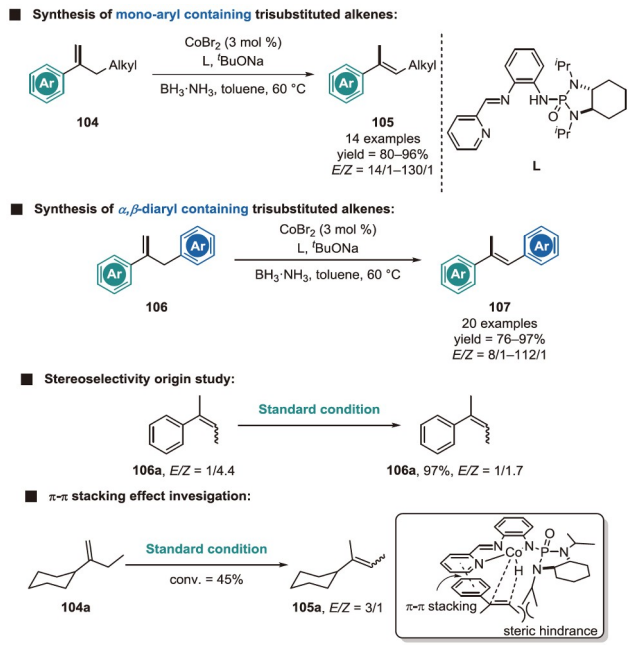

Scheme 36 Cobalt-catalyzed alkene stereoselectivity isomerization *via* π-π stacking interactions (color online).

but *Z* isomer remained the predominant product, suggesting that the stereoselectivity of the reaction should be derived primarily from the isomerization of the terminal to internal alkenes rather than the isomerization of *E*/*Z* isomers of the trisubstituted alkene product. In the absence of aryl substituents, stereoselectivity (*E*/*Z* = 3/1) is significantly reduced. This finding demonstrated that π-π stacking interactions may have contributed to the selectivity and efficiency of the reaction.

Iron hydride insertion/elimination pathway. Iron catalyst methods, which have fewer negative environmental and toxicological impacts, have also proven critical in this area. Huang *et al*. [60] in 2021 employed an iron complex comprising a phosphine-pyridine-oxazoline (PPO) ligand to isomerize *α*-substituted styrenes **108** to trisubstituted olefins **109** (Scheme 37). Since the catalytic system was effective for 1,1-disubstituted olefins with both electron-withdrawing and electron-donating groups on the aryl ring, it provided a feasible synthesis approach for monoaryl and *α*,*β*-diaryl containing trisubstituted alkenes. Crossover and radical capture experiments ruled out the concerted H-transfer and H-atom transfer processes. Most likely, the isomerization reaction proceeded *via* the reversible iron hydride insertion and *β*-H elimination pathway.

The same group created a new pincer-ligated Fe catalyst (Scheme 38) [61] for the widely used *Z*-selective isomerization of 1,1-disubstituted alkenyl boronates **110** to trisubstituted alkenes **111**. The stereoselectivity could be improved by using the phosphine-pyridine-imidazoline (PNN_{imid}) ligand by increasing the steric hindrance around the Fe center. The *Z*-selectivity is influenced by the steric effect that occurs during the *β*-H elimination process. Using different ratios of $[Fe]Cl_2$ and $NaBHEt_3$, multiple iron hydride catalysts were produced, according to *in situ* solvent-assisted electrospray ionization mass spectrometry (SAESI-MS) experiments. The above two catalysts were separately effective for different substrates. The dihydride $(PNN_{imid})FeH_2$ is a favorable catalyst for the formation of sterically more demanding aryl-substituted products **113**, while the monohydride (PNN_{imid})FeHCl is effective for the synthesis of less hindered alkyl-bearing trisubstituted *Z*-alkenyl boronates **111**.

2.3.2 *Carbocation mechanism*

The acid-catalyzed isomerization of alkenes *via* a carbocation mechanism has also been developed as an alternative method. Despite its widespread use in cyclic alkene systems, stereoselective isomerization of acyclic alkenes is extremely difficult due to acid-induced alkene dimerization. A hidden Brønsted acid catalyst was used by Yu *et al*. [62] in 2021 to achieve a highly stereoselective positional isomerization of acyclic alkenes **114** (Scheme 39). Under $Al(OTf)_3$ catalyzed conditions, a wide variety of *α*-alkyl substituted styrenes **114** were converted into stereo-defined tri- or tetra-substituted alkenes **115** featuring one or two aryl groups, and *E*-selectivity was found as a result of the steric effect during the deprotonation process. The stereoselectivity decreased to some extent for electron-rich styrene substrates. Deuterium-labeling experiments indicated that the protonation and deprotonation processes are potentially reversible. In addition, several control tests indicated that a trace amount of Brønsted acid (HOTf) produced *in situ* can prevent alkene dimerization. Despite the effectiveness of this ionic isomerization strategy, the stereoselective synthesis of triarylsubstituted and 1,1-diaryl-containing trisubstituted alkenes has not yet been accomplished. Internal alkenes are not exposed; hence it appears that this approach is primarily useful for terminal alkenes.

2.3.3 *Radical mechanism*

Radical isomerization is another method for producing trisubstituted alkenes containing an aryl group. It is critical to inhibit the second H radical transfer, which is usually faster than the first, to induce isomerization rather than hydrogenation. Norton *et al*. [63] employed $Co(dmgBF_2)_2(THF)_2$ as a catalyst under H_2 pressure to overcome this problem by producing a low concentration of a H radical donor, with a

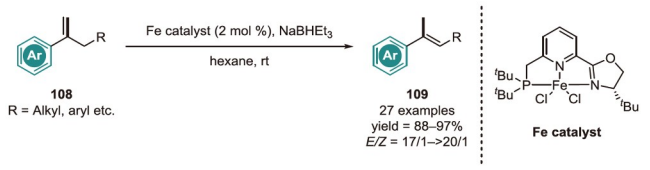

Scheme 37 Iron-catalyzed alkene stereoselectivity isomerization (color online).

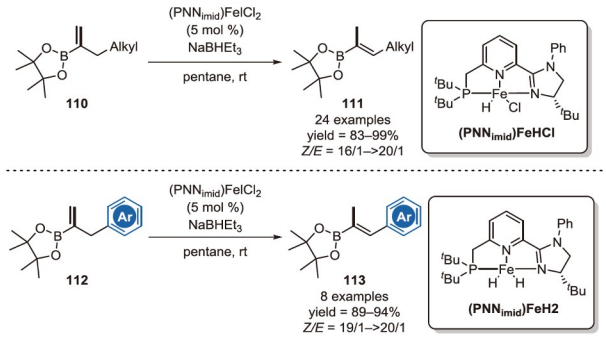

Scheme 38 *Z*-selective isomerization of 1,1-disubstituted alkenyl boronates to trisubstituted alkenes (color online).

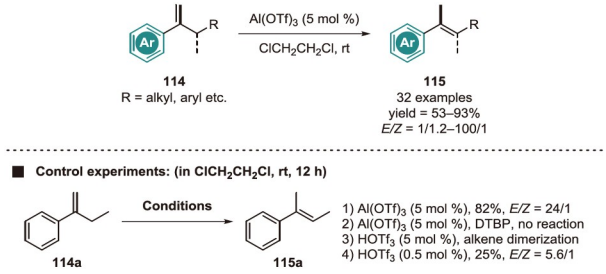

Scheme 39 Al catalyzed alkene stereoselectivity isomerization (color online).

negligible rate of the second transfer (Scheme 40). This method isomerized the terminal double bond of substrate **116a**, rather than the benzyl double bond. Furthermore, the stereoselectivity of isomerization still needs to be enhanced.

2.3.4 1,3-Hydrogen atom transfer (HAT) mechanism

Although the aforementioned three strategies are effective for synthesizing trisubstituted alkenes *via* an isomerization process, hydrogen scrambling and stereoselectivity are challenging to be regulated. In contrast to these mechanisms, the radical-induced 1,3-H shift provided a concerted hydrogen transfer isomerization pathway. Internal H shift is driven by an inherent driving force in the metalloradical-substrate complex. Schoenebeck *et al.* [64] accomplished intramolecular 1,3-hydrogen atom relocation to produce *E*-alkenes **119** by employing dimeric Ni(I) complexes to generate open-shell monomers, which rapidly captured H radicals and complexed with alkene substrates to convert hydrogen transfer into an intramolecular process (Scheme 41). The 1,3-H shift only took place intramolecularly, according to the crossover experiment. According to the computational analysis, no stable intermediates were produced, resulting in insufficient time for exchange processes.

2.4 Selective cleavage of carbon-fluorine bonds

In this subject, trisubstituted alkenes can be produced utilizing two distinct substrates. The first is *gem*-difluoroalkenes, which are commonly utilized in the synthesis of fluorine-containing trisubstituted alkenes. The second is monofluoroalkenes, which are a valuable synthon for producing trisubstituted alkenes containing only carbon atoms. Four primary strategies have been established and are discussed in the next section.

2.4.1 Nucleophilic vinylic substitution (S_NV) mechanism

S_NV is a useful approach for synthesizing multisubstituted alkenes, which is often performed by an addition-elimination mechanism. The monofluoroalkene S_NV reaction is a highly effective method for the stereoselective synthesis of trisubstituted alkenes.

S_NV of trisubstituted fluoroalkenes to construct the carbon-hetero bonds. Compared with difluoroalkenes, monofluoroalkenes exhibited less reactivity, and ester groups were frequently employed to activate the double bond. Based on this approach, Tsui *et al.* [65] developed an S_NV reaction for the synthesis of vinylic heteroatom-substituents-bearing trisubstituted alkenes **122** from (*E*)-*β*-monofluoroacrylates **120**. Nucleophiles with O/N/S atom performed well, and alkenes containing aryl or benzyl substituents were also compatible (Scheme 42). The stereo-control of the alkene geometry is complete, allowing only (*E*)-products to be formed. The formation of intramolecular hydrogen bonds between the ester enolate and the *β*-site hydrogen atom is a probable explanation for the stereocontrol in the addition-elimination pathway. Consequently, bond rotation is restricted until *β*-F elimination occurs, permitting the generation of (*E*)-products.

S_NV of trisubstituted fluoroalkenes to construct the carbon-carbon bonds. Grignard reagents **124** were also effective in the S_NV reaction of monofluoroalkenes **123** with excellent selectivities, hence facilitating the synthesis of stereo-defined trisubstituted alkenes **125** [66]. Ester groups-bearing diaryl or arylalkyl trisubstituted alkenes were synthesized using this approach, which was compatible with aryl and alkyl Grignard reagents (Scheme 42).

2.4.2 Migratory insertion/β-F elimination mechanism

This method of fluoroalkene synthesis was shown to be feasible by the migratory insertion of transition metal into *gem*-difluoroalkenes. The inherent feature of *gem*-difluoro substituents was responsible for the regio- and stereo-se-

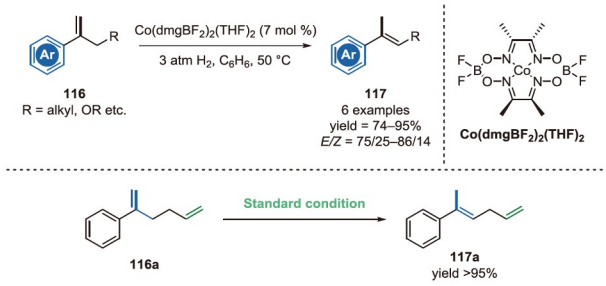

Scheme 40 Cobalt catalyzed isomerization of alkenes *via* a radical mechanism (color online).

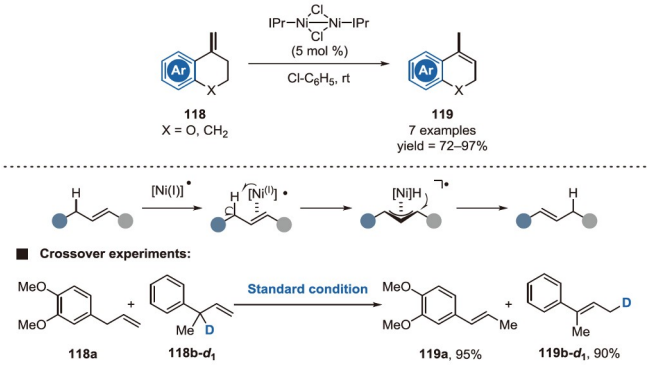

Scheme 41 Isomerization of alkenes *via* intramolecular 1,3-hydrogen atom relocation (color online).

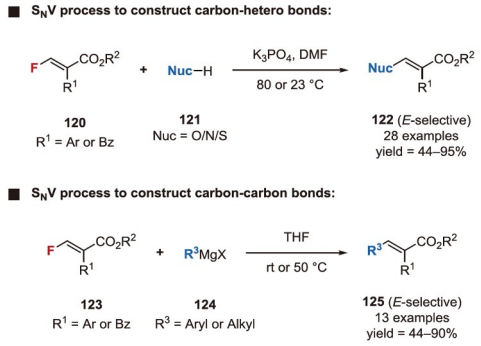

Scheme 42 S_NV of trisubstituted fluoroalkenes (color online).

lectivity. In addition, it is relatively rare to synthesize trisubstituent alkenes utilizing monofluoroalkenes as substrates *via* this mechanism.

Transmetallation/migratory insertion/β-F elimination sequence. Toste *et al*. [67] explained the palladium-catalyzed defluorinative coupling of aryl-substituted *gem*-difluoro-alkenes **127** with aryl boronic acids **126** to yield highly stereoselective monofluoroalkenes **128** (Scheme 43). A rare instance of *β*-F elimination from alkyl-palladium intermediates **M26** was described, giving a redox-neutral mechanism that required neither the addition of external oxidants nor base. When 1,1-difluoro-1,2-dipheneylethane **129a** was treated under standard reaction conditions, the corresponding mono-fluoroalkene **128a** could not be produced, proving that the *β*-fluoride elimination is likely mediated by a palladium alkyl intermediate rather than being solely base-mediated.

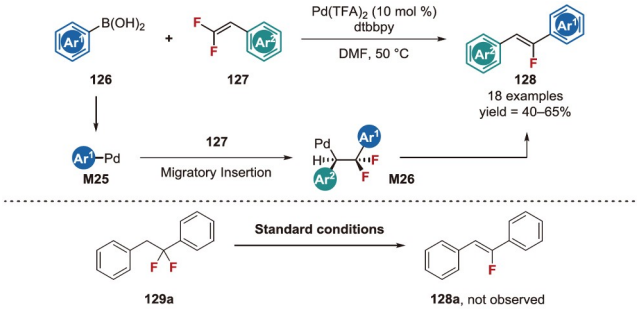

Scheme 43 The palladium-catalyzed defluorinative coupling of aryl-substituted *gem*-difluoroalkenes (color online).

Recently, Tsui *et al*. [68] describe a highly selective Rh(I)-catalyzed defluorinative coupling of boronic acids **130** with (*E*)-*β*-monofluoroacrylates **129** and **132**. In comparison to the S_NV reaction, there is an inversion of double bond geometry. The ligand BINAP was crucial for the reactivity as well as the geometry of the double bond in aryl-substituted substrates (**129**). The DPPB, on the other hand, was applicable to benzyl-substituted substrates. Substituents in the *ortho* position increased reaction times and decreased stereoselectivity. A series of mechanistic studies and DFT simulations demonstrate that the *syn*-migratory insertion of aryl rhodium species and the *syn*-*β*-F elimination are responsible for the stereoselectivity of product. Deuterated **132a-D** yielded product **133a-D** with complete retention of D, indicating that no H/D exchange processes occurred in the reaction pathway (Scheme 44).

C(sp^2)–H bond activation/migratory insertion/β-F elimination sequence. In rhodium-catalyzed reactions, the activation of the carbon-hydrogen bond can trigger the carbon-fluorine bond cleavage. In 2015, Loh *et al*. [69] reported a highly effective approach for C–H/C–F bond activation by rhodium^{III}-catalyzed *α*-fluoroalkenylation of (hetero)arenes **134** (Scheme 45). This method was applicable to indole and substituted aromatic rings as well. The pyridine, pyrimidine, and amide proved to be effective directing groups for commencing the C–H bond activation pathway. In addition, the activation of the C–F bond *via* the formation of hydrogen bonds was important for the success of this transformation, whereas the addition of external bases to neutralize the H–F produced in the reaction was detrimental to its success.

C(sp^3)–H bond activation/migratory insertion/β-F elimination sequence. The pathway can also be initiated by the C(sp^3)–H bond activation. Wang and Li *et al*. [70] achieved mild and redox-neutral conditions for the benzylic C–H bond activation/*α*-fluoroalkenylation of 8-methylquino-lines **137** with *gem*-difluorostyrenes **138**. As a result, numerous monofluoro *Z*-olefins **139** (Scheme 46) were synthesized.

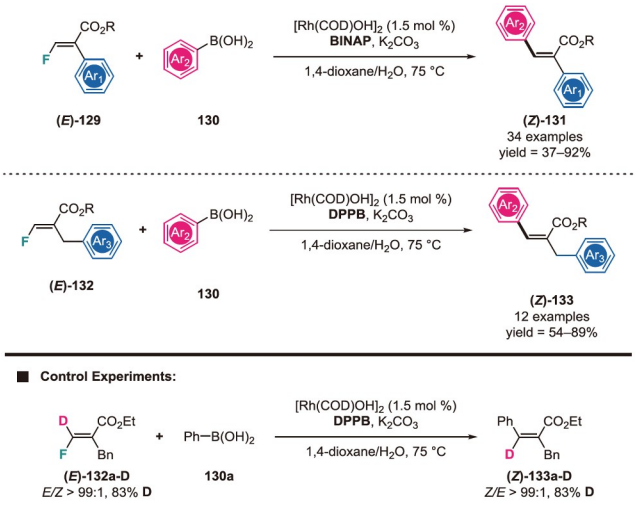

Scheme 44 The Rh-catalyzed defluorinative coupling of fluoroalkenes (color online).

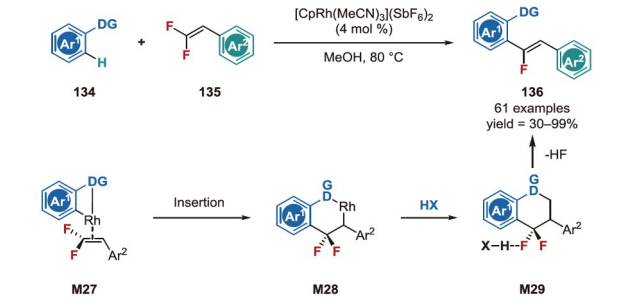

Scheme 45 Rh-catalyzed α-fluoroalkenylation of (hetero)arenes through C–H/C–F bond activations (color online).

The H/D exchange study suggested that the C−H bond activation was essentially irreversible, and the simultaneous kinetic isotope study showed that the breaking of the methyl C−H bond was probably involved in the turnover-determining step.

2.4.3 *Radical addition mechanism*

Fluorine-containing arylalkyl alkenes can be synthesized using a new approach involving the radical addition of *gem*-difluoroalkenes. Gong and Fu *et al.* [71] developed this method by combining fluorine chemistry and reductive cross-coupling reactions (Scheme 47). $C(sp^2)$–$C(sp^3)$ bonds were constructed by reacting sterically hindered secondary and tertiary alkyl halides **141** with *gem*-difluoroalkenes **140** using $(Bpin)_2/K_3PO_4$ as the terminal reductant. Additionally, a good functional group tolerance and an acceptable *Z*-selectivity were found. According to the radical clock experiment, alkyl halides were inserted into fluoroalkenes using the radical addition mechanism. Under standard reaction conditions, *gem*-difluoroalkane **143b** did not produce the desired product, excluding the base-mediated β-F elimination. Control-studies also ruled out the *in situ* Suzuki coupling

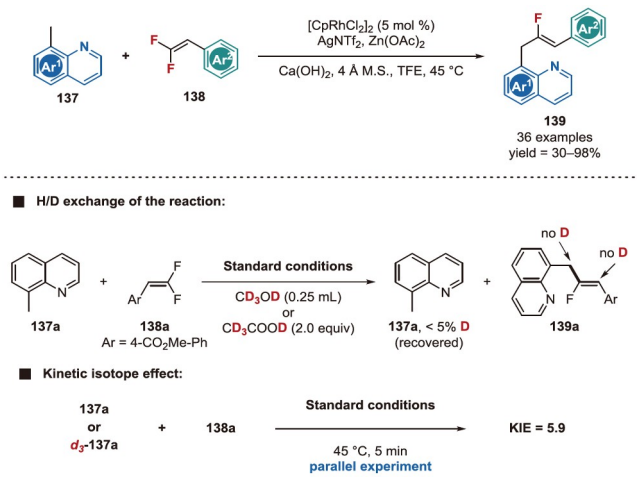

Scheme 46 Rh-catalyzed benzylic C–H bond activation/α-fluoroalkenylation (color online).

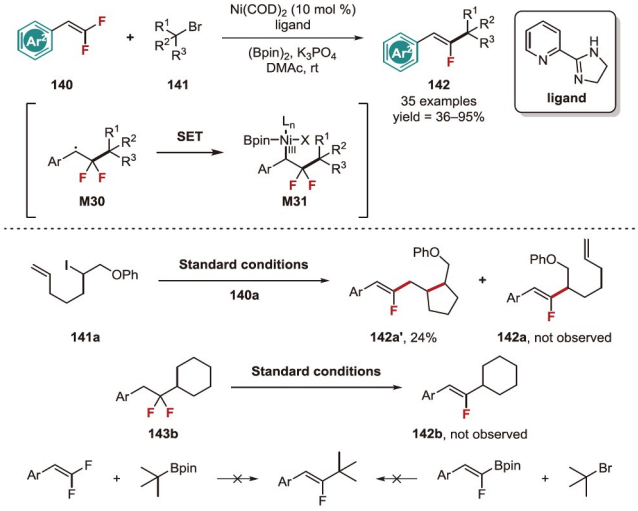

Scheme 47 Radical addition of *gem*-difluoroalkenes (color online).

mechanism. The authors also suggested that the synthesis of intermediate **M31** could promote stereoselectivity.

In contrast to the previous result, Nambo and Crudden *et al.* [72] reported the desulfonylative radical addition of tertiary alkyl groups to *gem*-difluoroalkenes **145** by photoredox Ir-catalysts (Scheme 48). Thermodynamically unfavorable *E*-fluoroalkenes were produced and then used to facilitate the subsequent *Z*/*E* isomerization by a triplet-triplet energy transfer process. Under visible-light irradiation, a photo-excited Ir^{III} complex was reduced to the corresponding Ir^{II} species, which then reacted with alkylsulfone **144** to form alkyl radical **M33** *via* the SET process. The radical **M33** was then added to the *gem*-difluoroalkene substrates **145** to produce intermediate **M34**. A second Ir-mediated SET produced the anionic molecule **M35**, which, upon fluoride elimination, resulted in the formation of the thermodynamically stable *Z*-isomer **147**. Finally, the first produced

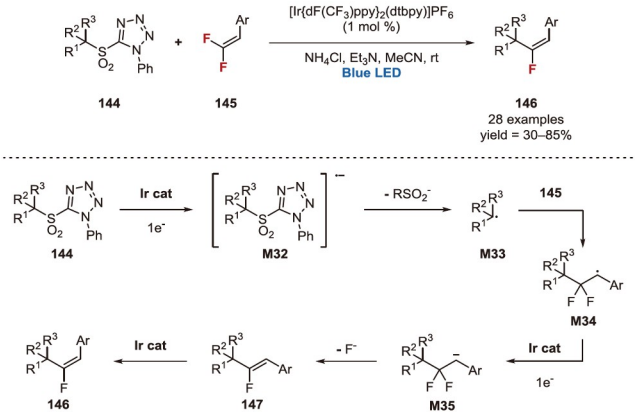

Scheme 48 The desulfonylative radical addition of tertiary alkyl groups to *gem*-difluoroalkenes (color online).

Z-isomer was isomerized to generate the less stable *E*-isomer **146** as the major product through energy transfer process from the Ir catalyst.

2.4.4 C−F bonds activation mechanism

Oxidative addition of C−F bonds. The transition-metal catalyzed hydrodefluorination (HDF) of *gem*-difluoroalkenes could result in the production of valuable terminal monofluoroalkenes. Tsui *et al.* [73] established a highly stereoselective palladium-catalyzed HDF method for the synthesis of trisubstituted monofluoroalkenes **150** in 2020 (Scheme 49). The findings revealed that an ester substituent on the alkenyl group was essential because it served as a dual role. The ester substituent not only activated the carbon-fluorine bond but also acted as a directing group, promoting stereoselectivity. Alkyl- or aryl-substituted *gem*-difluoroalkenes were effective substrates; however, aryl substituted substrates required room temperature with 5 mol% TsN_3 as an additive to prevent the formation of an "over-reduced" side product. A series of investigations showed that azide compounds interacted with the triphenylphosphine ligand of $Pd(PPh_3)_4$ to form coordinated unsaturated $Pd(PPh_3)_2$, which served as the active species for the C−F bond oxidative addition process.

Cleavage of C−F bonds via photoredox and hydrogen-atom-transfer catalysis. Alkenyl radicals and fluoride ions can be produced when C−F bonds are broken in the presence of a photocatalyst. Alkyl radicals can capture this sequence to complete the cross-coupling reaction between radicals. Although this approach is frequently employed to synthesize tetra-substituted fluoroalkenes by employing *gem*-difluoroalkenes as substrates, there are a few examples involving trisubstituted fluoroalkenes.

In 2019, Wang *et al.* [74] investigated a visible-light photoredox-catalyzed combining HAT approach for the monofluoroalkenylation of inert C(sp^3)−H bonds. In this review, the authors have focused on tetra-substituted fluoroalkenes and have only provided four examples of trisubstituted fluoroalkenes **156**. The unsatisfactory stereoselectivity of this reaction can be attributed to the rapid recombination of fluoroalkenyl radicals, which makes their control difficult. Scheme 50 depicts a specific reaction mechanism. HAT process produced alkyl radicals and fluoroalkenyl radicals was generated in the presence of Ir^{II} catalyst. Following radical-radical cross-coupling terminated the reaction effectively.

Deng *et al.* [75], however, broadened this field by investigating various types of inert C(sp^3)−H bond fluoroalkenylation employing $Ir(dFCF_3ppy)_2(dtbbpy)PF_6$ as the photocatalyst and Bu_4NBr as the HAT catalyst. Scheme 51 depicts some representative substrates, and the mechanism of this reaction is comparable to Wang's study (Scheme 50). Unfortunately, the issue of stereoselectivity has not yet been resolved.

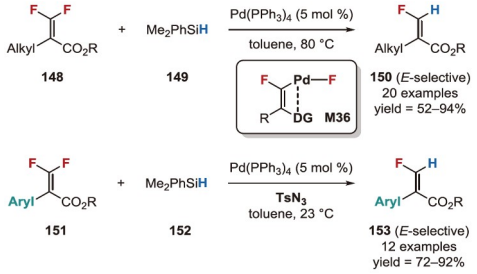

Scheme 49 HDF process for the synthesis of trisubstituted monofluoroalkenes (color online).

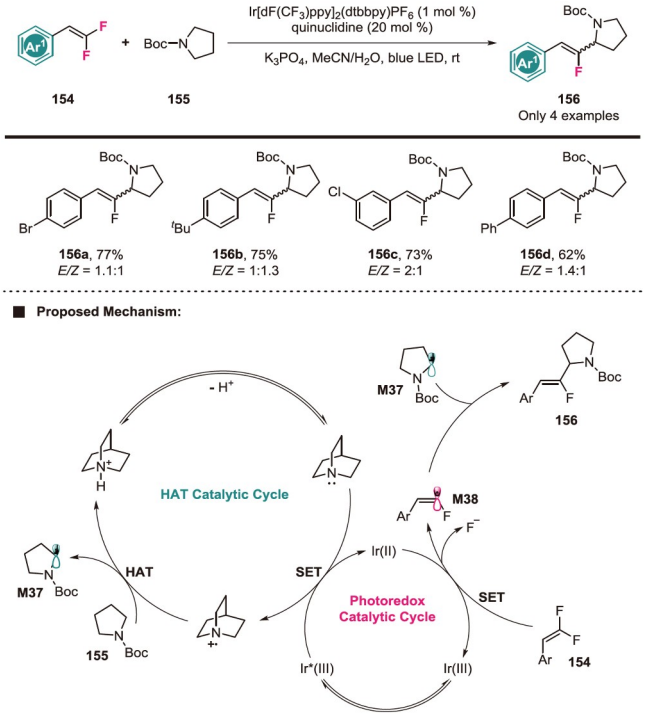

Scheme 50 Synthesis of trisubstituted fluoroalkenes *via* photoredox and HAT process (color online).

2.5 Stereodivergent synthesis of trisubstituted alkenes

Several aforementioned strategies have yielded an abundance of tools for the stereoselective synthesis of trisubstituted alkenes; however, stereodivergent synthesis is a more feasible method for synthesizing *Z*- and *E*-alkenes simultaneously.

2.5.1 Substrate-controlled stereodivergent synthesis

Terminal alkyne insertion involving three-component reactions. A three-component procedure could be employed to effectively synthesize a series of stereo-defined 1,1-diaryl trisubstituted alkenes. Terminal alkynes **160** were carboperfluoroalkylated with perfluoroalkyl iodide **162** and aryl boronic acids **161** in the presence of palladium catalysis [76]. Alkenes with various geometries were synthesized by changing the aryl substituents in both the alkynes and boronic acids components. All reactions were carried out with complete regioselectivity and high stereoselectivity towards the *anti*-addition product. The results of various mechanistic studies indicated that this protocol involves Pd^0/Pd^I and Pd^0/Pd^{II} cycles. Internal alkynes have also been proven to be suitable substrates for synthesizing tetra-substituted alkenes (Scheme 52).

C−H bonds activation involving aryl to vinyl metal migration reactions. Various stereo-defined 1,1-diaryl trisubstituted and triarylsubstituted alkenes can be synthesized by aryl to vinyl metal migration reactions. The geometry of the double bond can be effectively modified by varying the position of the TDG, which was systematically introduced in the previous section (as depicted in Scheme 12) [31,32].

2.5.2 Catalytic system-controlled stereodivergent synthesis

Photocatalyst-controlled triplet-triplet energy transfer (ET) process involving isomerization of alkenes. Rueping *et al.* [77] developed a three-component arylacetylene difunctional-lization reaction (Scheme 53). Both *E*- and *Z*-isomers of trisubstituted alkenes can be synthesized by using a photocatalyst with an appropriate triplet state energy. In this procedure, a radical precursor reacted with the Ni^I complex by a SET process, and a *syn*-migratory insertion of the Ni^I species into alkynes was observed, as well as a Ni-assisted *anti*/*syn* isomerization of alkenyl nickel intermediates that produced $\mathbf{P_{anti}}$ as the main product [7]. The triplet state energy of the photocatalyst E_T(**PC**) controlled the subsequent isomerization process of the generated product. The *anti*-addition product ($\mathbf{P_{anti}}$) was synthesized without the need for a subsequent isomerization step when $E_T(\mathbf{PC}) < E_T(\mathbf{P_{anti}})$. When $E_T(\mathbf{P}_{syn}) > E_T(\mathbf{PC}) > E_T(\mathbf{P_{anti}})$, effective isomerization was found, with $\mathbf{P_{syn}}$ being the predominant isomeric product. As demonstrated in the figure below, Ir-based photocatalyst **2** produced *syn*-addition alkenes as the major product (*Z*/*E* = 89:11), whereas Ru-based photocatalyst **3** achieved a *Z*/*E* ratio of 1:99. However, using photocatalyst **1** alone resulted in poor stereoselectivity (*Z*/*E* = 62:38) because of the high triplet state energy ($E_T(\mathbf{PC}) > E_T(\mathbf{P}_{syn}) > E_T(\mathbf{P_{anti}})$). This method provided an option for substrates incapable of adjusting stereoselectivity by steric effect.

Controlled triplet-triplet ET process by switching between electrochemistry and photocatalysis. As previously described, the triplet-triplet ET approach has proven to be a highly effective method for producing high levels of stereoselectivity [78]. The ET process can be efficiently avoi-

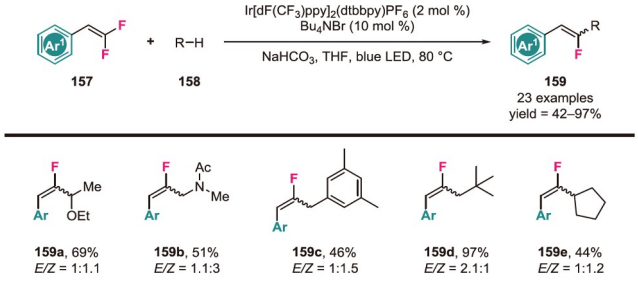

Scheme 51 Inert C(sp^3)−H bond fluoroalkenylation (color online).

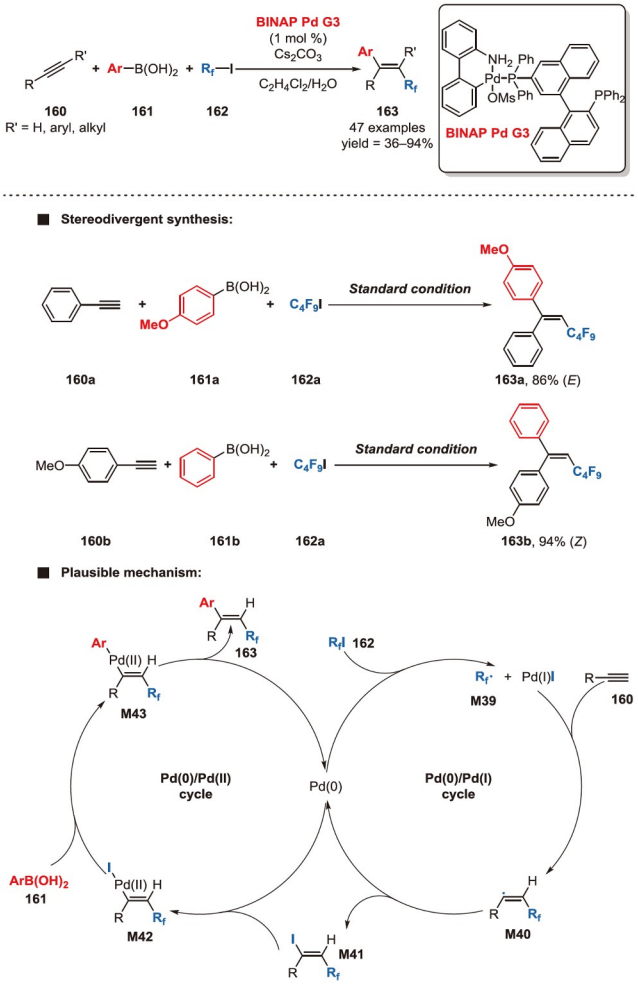

Scheme 52 Terminal alkyne insertion involving three-component reactions (color online).

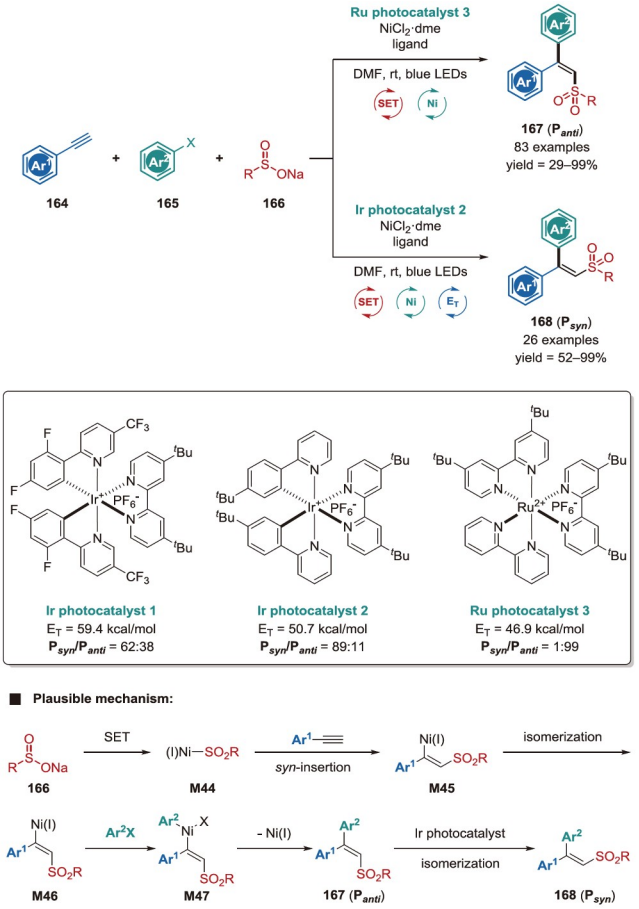

Scheme 53 Photocatalyst-controlled triplet-triplet energy transfer (ET) process involving isomerization of alkenes (color online).

ded with electrochemical technology. Stereo-defined 1,1-diaryl trisubstituted alkenes could be synthesized selectively by photochemical or electrochemical processes using arylacetylenes **169**, aryl bromides **170**, and alkyl bromides **171**. When the reaction was carried out with electricity and nickel, only the *E* isomer (*anti*-insertion) was formed; however, the *Z* isomer (*syn*-insertion) was formed with high stereoselectivity when photo- and nickel dual catalysts were used. In addition, photocatalysts were not required to produce *Z*-trisubstituted alkenes under photo-assisted electrochemical conditions. The nickel-based SET process in this reaction produced the carbon radical that offered enhanced regioselectivity and contributed to the synthesis of a single product *via* an *anti*-insertion mechanism. The subsequent ET process or direct excitation results in *E*/*Z*-isomerization (Scheme 54).

3 Applications of triarylethene-based AIEgens

Since Tang *et al.* [9] first put forward the concept of AIE in 2001, AIE luminogens (AIEgens) have received increasing attention, not only because they overcome the drawbacks of

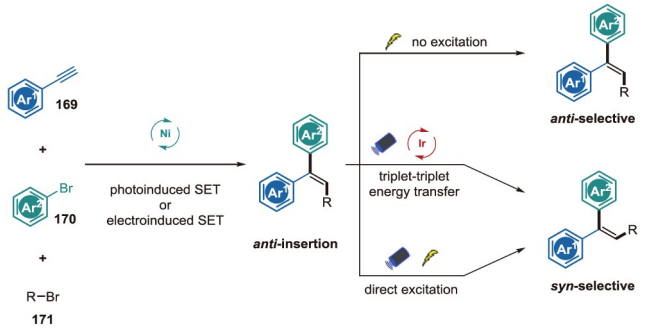

Scheme 54 Controlled triplet-triplet ET process by witching between electrochemistry and photocatalysis (color online).

aggregation-caused quenching (ACQ) of conventional fluorophores, but also because of their practical value [79] in the fields of light-emitting diodes [80–82], bioimaging [83–87], chemo-sensing [88–91], *anti*-counterfeiting [92] and so on. Among the established AIEgens, triarylethylene derivatives with simple molecular structures and fundamental applications have aroused extensive interests. In this section, the most significant applications of triarylethylene derivatives in optoelectronic devices, stimuli-responsive materials, sensors, therapies, and other fields over the past five years are reviewed.

3.1 Optoelectronic devices

Aggregation quenching appears to be a thorny issue in the development of optoelectronic devices, in which organic materials are normally used as solid thin films, and the formation of films is inherently accompanied by the onset of aggregation. It is thus highly desirable to develop luminescent materials that are capable of emitting intense light in solid form. Triarylethylene derivatives have been found to be promising emitters for the fabrication of advanced flexible integrated optoelectronic devices and circuits.

3.1.1 Optoelectronic organic semiconductors

Organic semiconducting materials with high electron mobility and robust luminescence are of both basic and practical importance for the advancement of organic optoelectronics. However, such ideal materials in solid state are uncommon due to a mismatch between the requirement for high charge transport provided by large coplanar conjugated structures and the conventional ACQ effect upon aggregation. In response to this, AIE molecules, triarylethylene-based semiconductors provide excellent device performance, which represent not only efficient photoluminescence quantum yield (PLQY) and satisfactory AIE effect, but also high hole mobility and large π-conjugation, showing great potential for high performance semiconductor devices.

Introducing building blocks with high electron mobility and superior chemo-/photostability into AIEgens is the

simplest and most effective strategy to fabricate devices with both AIE and exceptional optoelectronic properties. Gao and Tang *et al*. [93] reported an organic field-effect transistor (OFET) based on perylenediimide-substituted triphenylethylene (TriPE-*n*PDIs), among which TriPE-3PDIs showed the best performance in the reported near-infrared (NIR) AIEgen (quantum yield of 30% and electron mobility of over 0.01 $cm^2 V^{-1} s^{-1}$). By decorating PDI units with triphenylethene, both favorable intermolecular electron mobility and AIE characteristics were achieved. Compared with conventional AIEgen tetraphenylethylene (TPE), triphenylethene was chosen for its less crowded structure, greater molecular planarity and higher charge mobility (Figure 1). To evaluate the performance of the aforementioned molecules, thin film devices were fabricated and the critical role of film quality in OFET devices was proved. Furthermore, this AIEgen also may be potential in the future biological applications due to its NIR luminescence-related properties.

Anthracene was the first organic semiconductor discovered with electroluminescence property, which showed potential capacity for developing high mobility emissive organic semiconducting materials. Utilizing the same strategy above, Dong and Hu *et al*. [94] developed a novel organic compound 2-(2,2-diphenylethenyl)anthracene (DPEA) combined with half triphenylethylene and anthracene (Figure 2), which not only demostrated AIE behavior but also represented satisfied electrical charge transport characteristics. DPEA exhibited PLQY of 29.6% and hole carrier mobility of 0.66 $cm^2 V^{-1} s^{-1}$, which could be attributed to the dense molecular packing and compact intermolecular interactions in solid state.

3.1.2 Organic light-emitting diodes (OLEDs)

High-quality luminogens require not only high PLQY in film, but also high exciton utilization efficiency during the electroluminescence (EL) process. Blue organic light-emitting diodes (OLEDs) hold promise for full-color flat-panel displays and white lightnings [95–98]. However, the existing blue luminogens frequently suffer from aggregated quenching due to their massive π-conjugated structures [99–102]. Back to 2013, it was demonstrated that ACQ molecules could be converted into AIE molecules by integrating suitable motifs [103]. In 2016, Hu, Ye and Li *et al*. [104] first hypothesized that TriPE might be utilized instead of TPE to establish novel blue AIEgens because of their short conjugation lengths and the fact that some of them have blue-emitting capabilities inherently. Thereafter, Ma and Tang *et al*. [105] incorporated AIE groups tetraphenylethylene (TPE) or triphenylethylene (TriPE) with blue-emitted pyrene as examples to create OLED devices with both AIE features, electroluminescence (EL) properties and low turn-on voltages (Figure 3). However, the quantum efficiency in film (~0.03) and external quantum efficiencies (~1.07%) of Py-

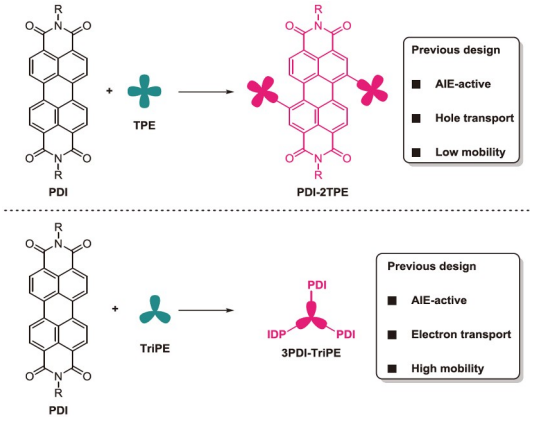

Figure 1 The design principles and structural comparison of tetraphenylethylene (TPE)/triphenylethene (TriPE)-based semiconductors [93] (color online).

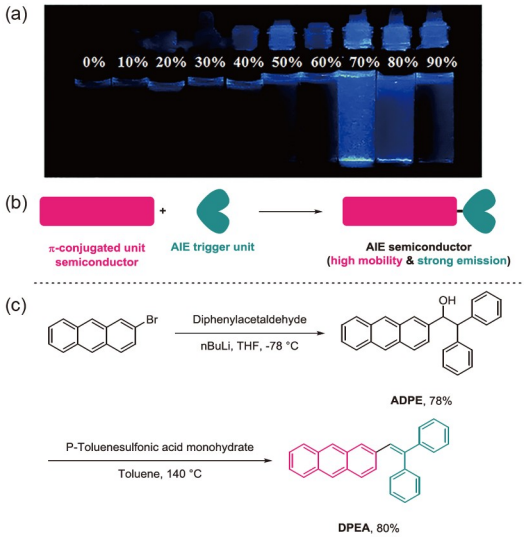

Figure 2 (a) Fluorescence photographs of DPEA solutions with different water contents (vol%) under illumination of a handheld UV (365 nm) lamp. (b) The design principle for an AIE active semiconductor that incorporate an AIE unit and a π-conjugated unit. (c) The synthetic procedures of DPEA [94] (color online).

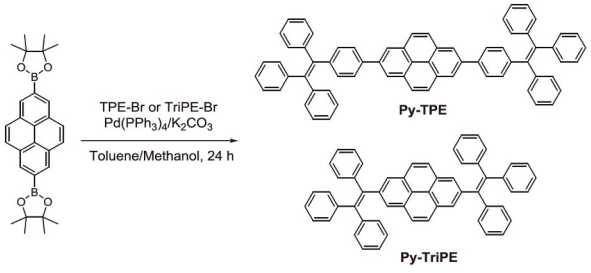

Figure 3 The synthetic route of the pyrene-based compounds Py-TPE and Py-TriPE [105].

TriPE were relatively poor and need to be improved.

Recently, Wang, Xu and Tang *et al*. [106] devised an efficient strategy to build superb nondoped blue OLEDs *via*

constructing high-lying charge-transfer (CT) state. They reported a nondoped blue AIEgen based on 2TriPE-BPI-MCN (Figure 4). Compared with its original matrix framework 2TriPE-BPI, 2TriPE-BPI-MCN with the insertion of *p*-cyano and *o*-methyl groups showed effective CT state, leading to strong triple-to-single conversion in the electroluminescence (EL) process, and maximum exciton utilization efficiency (EUE) about 50.2%. This review not only fabricated pure blue OLEDs with a CIE coordinate of (0.153, 0.147), but also gave the forecast that superior blue OLEDs may be achieved in future by engineering the energy levels of higher triplet states.

In addition to hybrid white OLEDs, single-molecular white-light luminogens also arouse great interests. Mei and Su *et al*. [107] achieved single-molecular white-light emission using AIE and VIE (vibration-induced emission) as two-pronged approach, filling a rare gap in the strategy of designing white light compounds with single-molecule. In this review, the adducted VIE-active DPAC and AIE-active triphenylethene (DPAC-Tri(*o*1,2)) were endowed with single-molecular white-light emission (CIE coordinates of (0.33, 0.31)) by changing the environment. Specifically, DPAC-Tri(*o*1,2) emitted tunable fluorescence from red to white and finally to blue as the degree of aggregation increased (*e.g.*, in a viscous solution or in the aggregated state).

3.2 Stimuli-responsive materials

Stimuli-responsive materials are "smart" materials that can produce rapid responses to a variety of external stimuli (including chemical, physical and biochemical stimuli) with different detectable signals, and have received increasing attention for their potential role as sensors [108–110], *anti*-counterfeiting [111–113], data storage [114], photoswitch [115,116], mechanochromic materials [117,118], *etc*.

However, it is not an easy task to create desirable responsive materials that are able to respond to external stimuli in a controllable and predictable pattern. The successful fabrication lies in the precise regulation on the molecular structures or on the intermolecular packing. As a matter of fact, AIEgens are likely to serve as smart materials compared to ACQ molecules because molecular aggregates allow for the modulation of intermolecular stacking and show appreciable fluorescent changes [119–125].

Research into photochromic and piezochromic materials that undergo reversible photo-/pressure-induced conversion between two or more states (such as crystalline or amorphous) has grown rapidly in recent years. Triarylethylene-based photochromism and piezochromism devices provide flexible chemical structures, striking photo-/piezochromic behaviors, high sensitivity response and speedy reaction time, offering new approaches for the novel applications of AIEgens.

3.2.1 *Photo-responsive materials*

After the first finding of tripheylethylene derivatives being AIE active, Chi *et al*. [126] have done a series of work to expand their applications in photochromism. In 2016, Luan, Zhang and Chi *et al*. [127] conducted a simple dichloro-substituted triphenylethylene derivative ($TrPECl_2$) that possessed both AIE and photochromic characteristics in solid state. The introduction of halogen atoms could enhance the ring-closing photochromic process. As anticipated, $TrPECl_2$ showed fast response to light irradiation with ON/OFF repeatability (Figure 5). Moreover, irradiation altered the morphology and wettability of $TrPECl_2$ microcrystalline surface. The photochromism of this material, however, could only be realized in solid state, and manageable reverted photochromic processes were also unattainable. Thus, a wider range (in solution or in thin films) and more controllable process of photochromism seem to be necessary. Thereafter, Yu, Zhang and Chi *et al*. [128] gave a report on the simple-structured thienyl containing triarylethylene derivatives (namely 2ThDpF and 3ThDpF) that showed the properties of photochromic behavior. A real-time and repeatable photoresponsive surface was fabricated based on 2ThDpF (Figure 6). This photoresponsive surface could not only be applied to solid state, but also to solution and

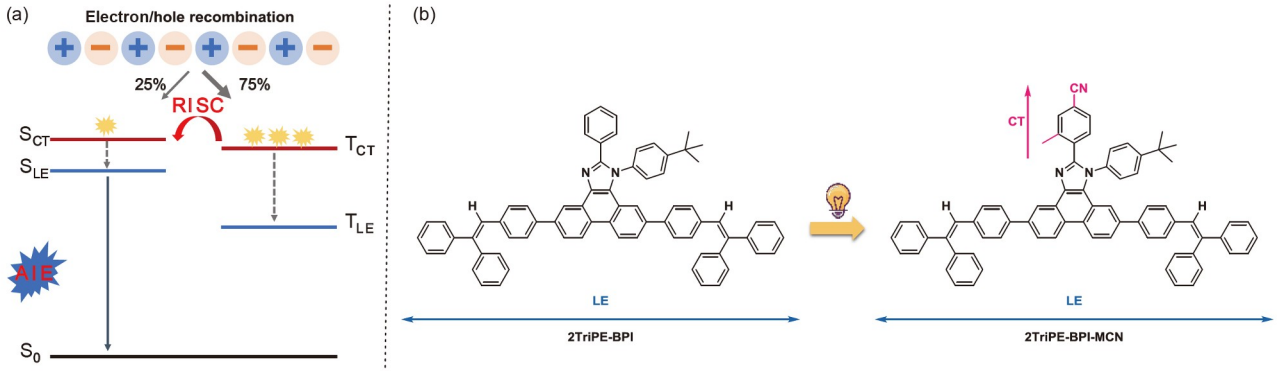

Figure 4 (a) Design strategy of blue luminogens proposed in the paper. RISC: reverse intersystem crossing. (b) Molecular designs of 2TriPE-BPI and 2TriPE-BPI-MCN [106] (color online).

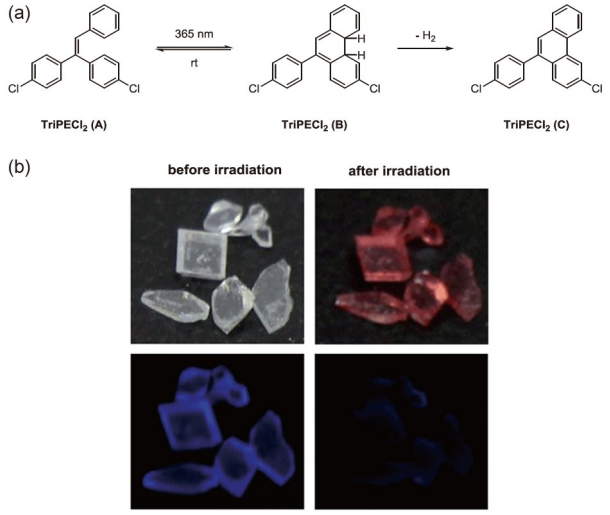

Figure 5 Proposed mechanism (a) and photographs (b) of the crystals of $TrPECl_2$ [127] (color online).

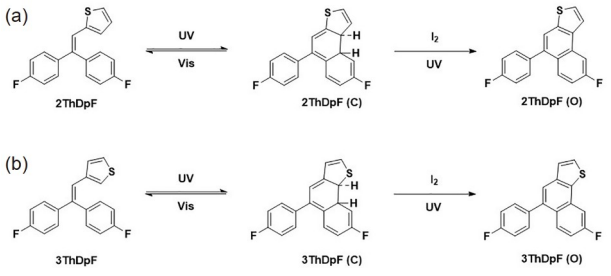

Figure 6 The photochromic mechanism of compounds **2ThDpF** (a) and **3ThDpF** (b) [128].

polymer film. Furthermore, the photochromic process is controllable in a short time, unlike the previously reported materials. Thus, upon UV-light irradiation, both the morphology and wettability of the photoresponsive surface changed drastically, while through white light irradiation, the morphology and wettability could be easily reverted. This property is extremely beneficial for the optoelectronic device fabrication, adsorption and biomedical engineering.

In addition to single photoresponsive systems, multiple photoresponsive systems, which can provide more than two states through optical control to enrich variety and diversity, high-order digital logic gates, and high-density optical memories, are receiving enormous attention and are crucial for advanced optical switching. Wang and Chi *et al*. [129] published a novel biphotochromic fluorescent switch N-2F derived from dithienylethene and triphenylethylene, two photochromic units. N-2F exhibits distinguished photochromic and fluorescent behaviors in tetrahydrofuran/water mixtures by changing the water ratio (f_w) under 254 and 500 nm light irradiations, corresponding to the cyclization and cycloreversion of dithienylethene and triphenylethylene (Figure 7). This review may provide new ideas for multifunctional materials.

3.2.2 *Pressure-responsive materials*

Along with photochromism, piezochromism has also drawn widespread attentions. However, when subjected to additional pressure, piezochromic materials usually display weak luminescence caused by pressure-induced π-π stacking. As a result, AIE materials may have the nature potential to develop innovative piezochromic materials. Jiang and Wang *et al*. [130] found that triphenylethylene (TriPE) exhibited both piezochromism behavior as well as conspicuous emission enhancement with pressure (0.0–0.8 GPa) upon compression (Figure 8). They also investigated the mechanism of the ring-opening reaction of the phenyl ring through *in situ* high-pressure infrared (IR) and angle-dispersive X-ray diffraction analysis, demonstrating the significant effect of intermolecular interactions on fluorescence properties.

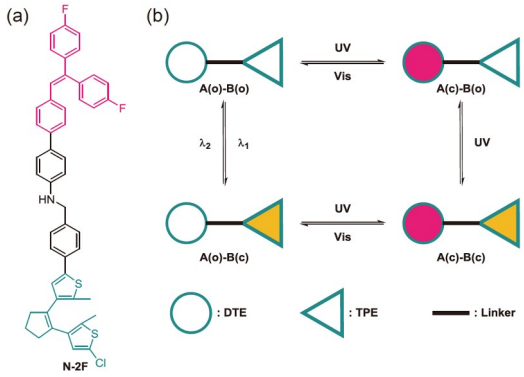

Figure 7 (a) Chemical structure of N-2F; (b) photochromic reactions of biphotochromic switch [129] (color online).

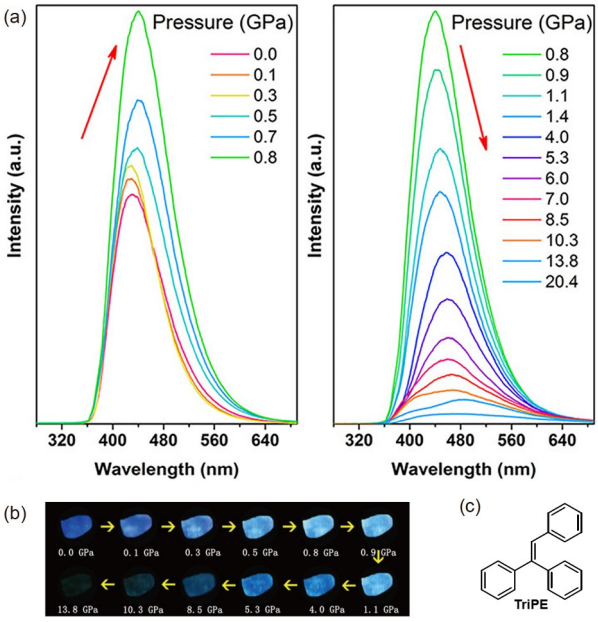

Figure 8 (a) PL spectra of a TriPE in the pressures range of 0.0−20.4 GPa. Change of the PL intensity represented by red arrows. (b) Corresponding PL photographs at different pressures. (c) The molecular structure of TriPE [130] (color online).

The introduction of the AIE concept has given a fresh impetus to the study of mechanoluminescent (ML) materials and a more in-depth exploration of their intrinsic mechanisms. Li *et al*. [131] developed a flexible and wearable ML device based on triphenylethylene-2-thiophene (tPE-2-Th), which combined AIE properties with self-assembly units, establishing the first quantitative relationship between pressure and ML intensity. This device gave a quick response to discontinuous force stimulus (in this case, human heartbeat), without the molecular structure being destroyed. Specifically, in this molecule, the triphenylethylene backbone served as the AIE group, while the thiophene rings were used to adjust the stacking form of the molecule in the crystal state *via* self-assembly under force stimulation to produce ML (Figure 9). After exploring the mechanism, the authors provided recommendations for fabricating efficient ML materials, opening up more opportunities to design preferable ML materials in the future.

In 2017, Zhang and Chi *et al*. [132] incorporated carbazole into a triphenylethylene derivative (TrPEBCar) to build an all-in-one molecule, which combined AIE, photochromic and piezochromic capabilities all together. They speculated that the electron withdrawing group in triphenylethylene could promote photochromism, while their rigid and bulky groups might cause a twisted packing mode in solid state, which would result in the occurrence of piezochromism (Figure 10). This is the first reported morphology-dependent photochromism, in which the photochromic properties were only observed in crystalline state rather than in pressing-/heating-induced amorphous state. Thus, pressure/heat could be utilized as gates to switch or control the photochromic properties. This mechanism offered a new approach for gated photochromic materials that functioned as both switch and indicator.

3.3 Sensors

3.3.1 Chemical sensing

Triarylethenes with asymmetrically substituted structures have the potential to enhance the luminescence when molecules aggregate (AIE effect). Furthermore, when these systems are electronically rich, they could easily interact with the electron-deficient systems. Because of this, triarylethenes of this type are well intented to enter the field of detecting explosives (including nitroaromatics and volatile organic compounds) and volatile organic polar solvents (such as acetone, acetonitrile, tetrahydrofuran, dichloromethane and trichlormethane).

Different from ACQ materials, AIEgens have many advantages for the efficient detection of explosives, including stronger emission in aqueous solutions and simpler development of solid-state devices [133]. In 2019, Tao and Huang *et al*. [134] gave new insights into chiral AIEgens. They published a triphenylethylene-based biimidazoles that not only exhibited AIE activity for the detection of explosives (including nitrobenzene (NB), 2-nitrotoluene (2-NT), 3-nitrotoluene (3-NT), 4-nitrotoluene (4-NT), 2,6-dinitrotoluene (2,6-DNT) and picric acid (PA)), but also helped to verify the relationship between the photophysical properties and orientational changes. They discovered that the detection performance for explosives in an aqueous medium depends on the alternation of the chiral configurations of triphenylethenes (Figure 11).

3.3.2 Biosensors

As for the AIE active triarylethylene, by conjugating selected binding heads with peripheral phenyl rings, the predetermined targets can be recognized specifically through the enhanced luminescence caused by binding induced aggregation. This phenomenon could be used as fluorescent/electrochemiluminescent sensors for detecting proteins, live bacteria, temperatures, viscosity, pH, *etc*.

Traditional methods of fluorescence detection for bacteria are mostly based on electrostatic adsorption, which has disadvantages such as altering bacterial states and failing to differentiate between live and dead bacteria. To address this

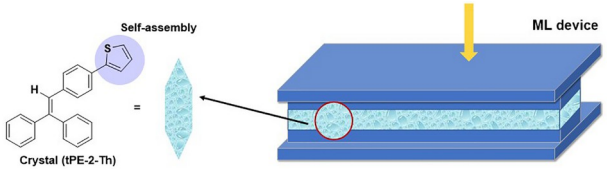

Figure 9 The molecular design and piezochromism behavior of novel ML materials [131] (color online).

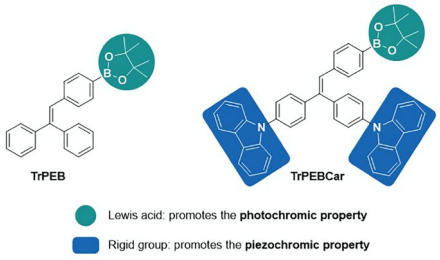

Figure 10 Molecular design strategy and chemical structures of compounds TrPEB and TrPEBCar [132] (color online).

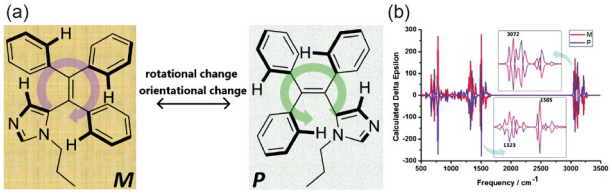

Figure 11 (a) 1-Propyl-5-(1,2,2-triphenylvinyl)-1*H*-imidazole has two rotational modes (M and P) of the benzene and imidazole rings; (b) calculated vibrational circular dichroism spectra of two chiral isomers (M and P) [134] (color online).

issue, Jin and Tang *et al*. [135] developed a biosensor for rapidly discriminating between live and dead bacteria through a new mechanism of mild complexation between phenylboronic acid *cis*-diols on bacterial surfaces. After conjugating phenylboronic acid onto triphenylethylene, the probe became AIE-functionalized and could be anchored to (both live and dead) bacterial surfaces to emit AIE luminescence. When combined with PI dyes, TriPE-3BA could distinguish between live and dead bacteria.

In addition to aggregation-induced luminescence mechanism, aggregation-induced electrochemiluminescence (AIECL) is investigated by Huang and Yang *et al*. [136]. AIECL has obvious advantages in opto-electrochemistry since it might prevent the low luminescent efficiency of organic materials in the solid state caused by ACQ. They described a label-free immunosensor for cardiac troponin I detection using the triarylethene derivative 4,4′-bis(2,2-diphenylvinyl)-1,1′-biphenyl (DPVBi). DPVBi was selected as a precursor with trimethylamine (TEA)/potassium peroxodisulfate ($K_2S_2O_8$) as a co-reactant to produce strong reductive-oxidative and oxidative-reductive ECL. Then, electro-deposited gold nanoparticles were designed to assist the construction of the label-free immunosensor (Figure 12). This system showed greater efficiency than the typical tetraphenylethylene and exhibited satisfied optoelectronic performance in practical sample analysis.

3.4 Therapeutics

In contrast to conventional photodynamic therapy (PDT)-employed photosensitizers (PSs), the unique aggregation lit-up fluorescence characteristic of AIEgens permits their vast bioimaging applications [137,138]. It was discovered that several triarylethylene-based AIEgens had aggregation enhanced reactive oxygen species (ROS) generating property, indicating their potential utilization in image-guided PDT.

Zheng, Jiang and Tang *et al*. [139] synthesized a bifunctional AIEgen, triphenylethylene-naphthalimide triazole (TriPE-NT) in 2018, to monitor and eradicate multidrug resistant (MDR) bacteria. The AIEgen is composed of two parts: the TriPE moiety imparts the system fluorescence to monitor drug-bacteria binding, while the NT moiety is utilized for antibacterial process. More importantly, the TriPE-NT permitted the generation of ROS under white light irradiation for further bacteria killing *via* PDT. AIE functionalized materials employed as PSs could successfully inhibit singlet state quenching and ROS reduction caused by aggregation, hence enhancing the efficacy of PDT. As an example of application, TriPE-NT effectively healed the wounds generated by various bacteria on rat models with negligible inflammatory reaction. This result showed the unlimited potential of AIEgens as a therapeutic agent in clinically relevant bacterial infections.

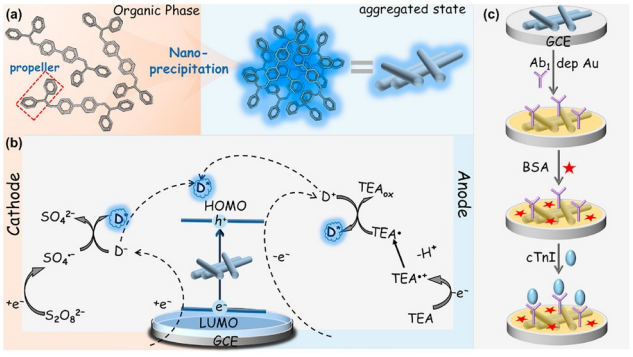

Figure 12 (a) The preparation process of DPVBi. (b) ECL mechanism of DPVBi nanobulks. (c) The fabrication process of the immunosensor [136] (color online).

4 Summary and outlook

For the last two decades, the AIE effect has been explored, and small organic compounds with varied structures have frequently been employed in this field. Although TPE has been widely explored, TriPE has received less attention. Due to the missing phenyl ring, the molecular architecture shows less molecular crowding, leading to an improvement in conjugation efficacy while retaining the AIE effect. The geometry of the double bonds in such molecules is a major factor in determining their characteristics. Therefore, it is necessary to continue developing stereoselective synthesis techniques for alkenes.

In the field of alkene synthesis, it is essential to select the right synthesis strategy based on the substantial structural changes between trisubstituted alkenes. The trisubstituted alkenes discussed in this paper are primarily involved in three types of substrates, including monoaryl-containing alkenes (1,2-dialkyl substituted and 1,1-dialkyl substituted), diaryl-containing alkenes (1,2-diaryl substituted and 1,1-diaryl substituted), and triaryl substituted alkenes. For the synthesis of 1,1-dialkyl substituted monoaryl alkenes, chelation-assisted alkenyl C−H bond arylation is an efficient route. And for 1,2-disubstituted monoaryl containing alkenes, Heck reaction and alkyne insertion are both feasible approaches. When the substrate contains an electron-withdrawing substituent, radical addition is also an alternative pathway. Methyl-containing trisubstituted alkenes can also be produced by the isomerization method. Heck reaction and alkenyl C−H bond activation yielded compounds with distinct geometries for 1,2-diaryl trisubstituted alkenes. Internal alkyne hydroarylation is another efficient technique. Isomerization and C−F bond cleavage are potentially viable options for some unique substrates. Both alkenyl C−H bond alkylation and alkyne insertion are efficient strategies for developing *gem*-diaryl trisubstituted alkenes. The synthesis of triaryl-substituted alkenes is usually difficult because of

the similar properties of the two aryl groups. Even while the Heck reaction and alkyne insertion can produce comparable products, the regioselectivity of these reactions frequently restricts their applicability. Alkenyl C−H bond activation appears to be the best choice, and the geometry of the double bond may be altered by adjusting the position of the DG (Scheme 55). Although the aforementioned methodologies may successfully solve the stereoselective synthesis of alkenes, it remains challenging to acquire a single geometric isomer for several unique TriPE skeletons that might be widely exploited in the materials, particularly for providing *Z* or *E* isomer, respectively. In follow-up research, it is necessary to design novel stereoselective synthesis methods around some practical trisubstituted alkenes. Furthermore, the stereo-convergent synthesis of a geometry defined trisubstituted alkene from the (*Z*,*E*)-mixed alkene substrate that deserves attention. In addition, it is also important to further develop stereo-divergent synthesis strategies to construct trisubstituted alkenes with different geometry structures simultaneously.

In the field of alkene application, the discovery of AIE solved the ACQ problem. After several years of vigorous development, AIE has been expanded beyond a simple optical phenomenon to a wide range of integrated disciplines, including physics, chemistry, materials, biology, and medicine. TriPE, exhibiting typical AIE properties, is a candidate backbone for potential applications due to its simple synthesis, flexible structure and variable conformation. However, the development of TriPE is still in its infancy compared to the TPE molecule, which has already become a widely used "star" backbone in the AIE field. While a number of systematic studies have been conducted in the field of optoelectronic devices and stimulus-responsive materials, applications in bioimaging and therapeutics are still in the preliminary stage.

Despite the impressive progress in the application of TriPE, there are still many unresolved issues and challenges.

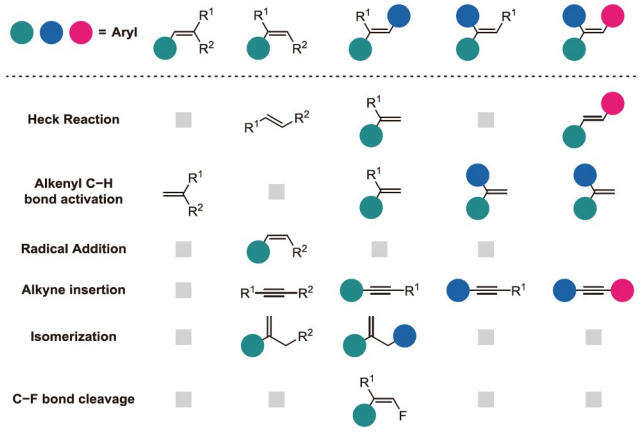

Scheme 55 Synthesis strategies of different types of trisubstituted alkenes (color online).

(1) Further development of TriPE-based photochromic materials with biocompatible properties (red or near-infrared light emission, water-solubility, *etc*.) is needed, and it is becoming a hot topic for biomedical applications such as cell imaging, drug chemotherapy, and drug delivery.

(2) Although the evidence has been presented to demonstrate that (*Z*)-TriPE and (*E*)-TriPE derivatives exhibit distinct chemical and physical properties, and their unique structural features have been used to design with (*Z*)-/(*E*)-selective conformations and to modulate the properties in aggregated states with different molecular stacking arrangements at this stage, applications based on the stereoselectivity of TriPE are rare. This may be due to several possible reasons: a) although the stereoselective synthesis of alkenes can be effectively addressed by the forementioned strategies, it is still difficult to obtain a single geometric isomer for some specific TriPE skeletons, which could be widely used in the materials field, especially for providing *Z* or *E* isomers, respectively. b) (*Z*)-/(*E*)-TriPE isomers are difficult to separate by using conventional purification operations (*e.g*., silica gel column chromatography), which also limits their applications. c) Confirming the stereochemistry of (*Z*)-/(*E*)-TriPE is challenging. The classic X-ray diffraction is reliable for confirming the geometry of stereoisomers only when they are easily grown as single crystals. Furthermore, photochromic isomerization also needs to be further confirmed during research process. d) At present, the AIE mechanisms of (*Z*)-/(*E*)-TriPE isomers are still yet to be clarified. In summary, the stereoselective synthesis, separation and application of TriPE are still to be developed.

(3) In some cases, the inherent selectivity of AIEgens is not satisfactory enough, and synthesis strategies that combine tunable and functional components into AIE cores by rational molecular design are needed to facilitate multifunctional applications, thus achieving high sensitivity, high selectivity, and high signal-to-noise ratio of AIE biosensors.

(4) Furthermore, expanding the application areas of TriPE requires more focus on molecular design. Guided by the application requirements, more multifunctional AIE materials can be designed in a targeted manner. There is still a lack of TriPE-based allosteric molecules with panchromatic emission in different external environments, pure organic materials with strong and long-lived phosphorescence at room temperature, and near-infrared fluorophores with high emission in aqueous environment *etc*., the simple construction of which are attractive but challenging tasks.

In conclusion, in the field of trisubstituted alkenes synthesis and application, a number of opportunities and challenges remain. We hope this review will help synthetic chemists navigate the systematic synthesis and related applications of trisubstituted alkenes to develop improved techniques and modifications of AIEgens with more application-appropriate structures. In addition, it allows material

and biochemical experts to determine the optimal synthesis pathway and appropriate skeleton.

Acknowledgements This work was supported by the National Natural Science Foundation of China (81874181, 21871284), the Major Scientific and Technological Special Project for "Significant New Drugs Creation" (2019ZX09301158), the Emerging Frontier Program of Hospital Development Centre (SHDC12018107), the Science & Technology Department of Shanghai (18401933500) and the State Key Laboratory of Bioorganic and Natural Products Chemistry. The authors would like to thank Shiyanjia Lab (www.shiyanjia.com) for the language editing service. Dedicated to the 70th Anniversary of Shanghai Jiao Tong University School of Medicine.

Conflict of interest The authors declare no conflict of interest.

1 Li J, Zhang Z, Wu L, Zhang W, Chen P, Lin Z, Liu G. *Nature*, 2019, 574: 516–521
2 Cuenca AB, Fernández E. *Chem Soc Rev*, 2021, 50: 72–86
3 Aïssa C. *Eur J Org Chem*, 2009, 2009: 1831–1844
4 Nguyen TT, Koh MJ, Mann TJ, Schrock RR, Hoveyda AH. *Nature*, 2017, 552: 347–354
5 Alisha M, Philip RM, Anilkumar G. *Eur J Org Chem*, 2022, 2022: e202101384
6 Neveselý T, Wienhold M, Molloy JJ, Gilmour R. *Chem Rev*, 2022, 122: 2650–2694
7 Bottcher SE, Hutchinson LE, Wilger DJ. *Synthesis*, 2020, 52: 2807–2820
8 Weiss J. *Nature*, 1943, 152: 176–178
9 Luo J, Xie Z, Lam JWY, Cheng L, Chen H, Qiu C, Kwok HS, Zhan X, Liu Y, Zhu D, Tang BZ. *Chem Commun*, 2001, 1740–1741
10 Niu G, Zhang R, Shi X, Park H, Xie S, Kwok RTK, Lam JWY, Tang BZ. *TrAC Trends Anal Chem*, 2020, 123: 115769
11 Liu H, Xiong LH, Kwok RTK, He X, Lam JWY, Tang BZ. *Adv Opt Mater*, 2020, 8: 2000162
12 Gao M, Tang BZ. *Coord Chem Rev*, 2020, 402: 213076
13 Ding D, Li K, Liu B, Tang BZ. *Acc Chem Res*, 2013, 46: 2441–2453
14 Zhao Z, Zheng X, Du L, Xiong Y, He W, Gao X, Li C, Liu Y, Xu B, Zhang J, Song F, Yu Y, Zhao X, Cai Y, He X, Kwok RTK, Lam JWY, Huang X, Lee Phillips D, Wang H, Tang BZ. *Nat Commun*, 2019, 10: 2952
15 Mei J, Hong Y, Lam JWY, Qin A, Tang Y, Tang BZ. *Adv Mater*, 2014, 26: 5429–5479
16 Leung NLC, Xie N, Yuan W, Liu Y, Wu Q, Peng Q, Miao Q, Lam JWY, Tang BZ. *Chem Eur J*, 2014, 20: 15349–15353
17 Yan D, Wu Q, Wang D, Tang BZ. *Angew Chem Int Ed*, 2021, 60: 15724–15742
18 Buttard F, Sharma J, Champagne PA. *Chem Commun*, 2021, 57: 4071–4088
19 La DD, Bhosale SV, Jones LA, Bhosale SV. *ACS Appl Mater Interfaces*, 2018, 10: 12189–12216
20 Zhang M, Zhao W. *Aggregate*, 2021, 2: e60
21 Nakashima Y, Hirata G, Sheppard TD, Nishikata T. *Asian J Org Chem*, 2020, 9: 480–491
22 Nilsson P, Larhed M, Hallberg A. *J Am Chem Soc*, 2001, 123: 8217–8225
23 Liu Y, Li D, Park CM. *Angew Chem*, 2011, 123: 7471–7474
24 Tsai JJ, Huang YH, Chou CM. *Org Lett*, 2021, 23: 9468–9473
25 Oi S, Sakai K, Inoue Y. *Org Lett*, 2005, 7: 4009–4011
26 Ilies L, Asako S, Nakamura E. *J Am Chem Soc*, 2011, 133: 7672–7675
27 Wencel-Delord J, Nimphius C, Patureau FW, Glorius F. *Chem Asian J*, 2012, 7: 1208–1212
28 Song S, Lu P, Liu H, Cai SH, Feng C, Loh TP. *Org Lett*, 2017, 19: 2869–2872
29 Li T, Shen C, Sun Y, Zhang J, Xiang P, Lu X, Zhong G. *Org Lett*, 2019, 21: 7772–7777
30 Shibata T, Kojima M, Onoda S, Ito M. *Org Lett*, 2021, 23: 8158–8162
31 Li MY, Han P, Hu TJ, Wei D, Zhang G, Qin A, Feng CG, Tang BZ, Lin GQ. *iScience*, 2020, 23: 100966
32 Zhang SS, Hu TJ, Li MY, Song YK, Yang XD, Feng CG, Lin GQ. *Angew Chem Int Ed*, 2019, 58: 3387–3391
33 Li M, Wei D, Feng C, Lin G. *Chem An Asian J*, 2022, 17: e202200456
34 Nakashima Y, Matsumoto J, Nishikata T. *ACS Catal*, 2021, 11: 11526–11531
35 Chen Y, Wang J, Wu X, Zhu C. *ACS Org Inorg Au*, 2022, 2: 392–395
36 Su MD, Liu YF, Nie ZW, Yang TL, Cao ZZ, Li H, Luo WP, Liu Q, Guo CC. *J Org Chem*, 2022, 87: 7022–7032
37 Yadav AK, Sharma AK, Singh KN. *Org Chem Front*, 2019, 6: 989–993
38 Suga T, Takada R, Shimazu S, Sakata M, Ukaji Y. *J Org Chem*, 2022, 87: 7487–7493
39 Ren S, Fu J, Cheng D, Li X, Xu X. *Tetrahedron Lett*, 2021, 66: 152829
40 Wu K, Sun N, Hu B, Shen Z, Jin L, Hu X. *Adv Synth Catal*, 2018, 360: 3038–3043
41 Kortman GD, Hull KL. *ACS Catal*, 2017, 7: 6220–6224
42 Oh CH, Jung HH, Kim KS, Kim N. *Angew Chem Int Ed*, 2003, 42: 805–808
43 Lautens M, Yoshida M. *Org Lett*, 2002, 4: 123–125
44 Lautens M, Yoshida M. *J Org Chem*, 2003, 68: 762–769
45 Kim N, Kim KS, Gupta AK, Oh CH. *Chem Commun*, 2004, 618–619
46 Arcadi A, Aschi M, Chiarini M, Ferrara G, Marinelli F. *Adv Synth Catal*, 2010, 352: 493–498
47 Liu Z, Derosa J, Engle KM. *J Am Chem Soc*, 2016, 138: 13076–13081
48 Zhu H, Xing J, Wu C, Wang C, Yao W, Dou X. *Org Lett*, 2022, 24: 4896–4901
49 Cacchi S, Fabrizi G, Goggiamani A, Persiani D. *Org Lett*, 2008, 10: 1597–1600
50 Xue F, Zhao J, Hor TSA. *Chem Commun*, 2013, 49: 10121–10123
51 Gao K, Lee PS, Fujita T, Yoshikai N. *J Am Chem Soc*, 2010, 132: 12249–12251
52 Zhou W, Yang Y, Wang Z, Deng GJ. *Org Biomol Chem*, 2014, 12: 251–254
53 Zhang J, Shrestha R, Hartwig JF, Zhao P. *Nat Chem*, 2016, 8: 1144–1151
54 Chen H, Gao L, Liu X, Wang G, Li S. *Eur J Org Chem*, 2021, 2021: 5238–5242
55 Liu X, Li B, Liu Q. *Synthesis*, 2019, 51: 1293–1310
56 Larionov E, Li H, Mazet C. *Chem Commun*, 2014, 50: 9816–9826
57 Liu H, Cai C, Ding Y, Chen J, Liu B, Xia Y. *ACS Omega*, 2020, 5: 11655–11670
58 Zhao J, Cheng B, Chen C, Lu Z. *Org Lett*, 2020, 22: 837–841
59 Zhang S, Bedi D, Cheng L, Unruh DK, Li G, Findlater M. *J Am Chem Soc*, 2020, 142: 8910–8917
60 Xu S, Liu G, Huang Z. *Chin J Chem*, 2021, 39: 585–589
61 Xu S, Geng P, Li Y, Liu G, Zhang L, Guo Y, Huang Z. *ACS Catal*, 2021, 11: 10138–10147
62 Hu X, He JX, Zhang Y, Zhou J, Yu JS. *Chin J Chem*, 2021, 39: 2227–2233
63 Li G, Kuo JL, Han A, Abuyuan JM, Young LC, Norton JR, Palmer JH. *J Am Chem Soc*, 2016, 138: 7698–7704
64 Kapat A, Sperger T, Guven S, Schoenebeck F. *Science*, 2019, 363: 391–396
65 Zong Y, Ma Q, Tsui GC. *Org Lett*, 2021, 23: 6169–6173
66 Wang Y, Tang Y, Zong Y, Tsui GC. *Org Lett*, 2022, 24: 4087–4092
67 Thornbury RT, Toste FD. *Angew Chem Int Ed*, 2016, 55: 11629–11632
68 Zong Y, Tang Y, Tsui GC. *Org Lett*, 2022, 24: 6380–6385
69 Tian P, Feng C, Loh TP. *Nat Commun*, 2015, 6: 7472

70 Kong L, Liu B, Zhou X, Wang F, Li X. *Chem Commun*, 2017, 53: 10326–10329
71 Lu X, Wang Y, Zhang B, Pi JJ, Wang XX, Gong TJ, Xiao B, Fu Y. *J Am Chem Soc*, 2017, 139: 12632–12637
72 Nambo M, Ghosh K, Yim JCH, Tahara Y, Inai N, Yanai T, Crudden CM. *ACS Catal*, 2022, 12: 9526–9532
73 Ma Q, Liu C, Tsui GC. *Org Lett*, 2020, 22: 5193–5197
74 Tian H, Xia Q, Wang Q, Dong J, Liu Y, Wang Q. *Org Lett*, 2019, 21: 4585–4589
75 Cao CL, Zhang GX, Xue F, Deng HP. *Org Chem Front*, 2022, 9: 959–965
76 Domański S, Chaładaj W. *ACS Catal*, 2016, 6: 3452–3456
77 Zhu C, Yue H, Maity B, Atodiresei I, Cavallo L, Rueping M. *Nat Catal*, 2019, 2: 678–687
78 Zhu C, Yue H, Rueping M. *Nat Commun*, 2022, 13: 3240
79 Yang J, Chi Z, Zhu W, Tang BZ, Li Z. *Sci China Chem*, 2019, 62: 1090–1098
80 Yang J, Huang J, Li Q, Li Z. *J Mater Chem C*, 2016, 4: 2663–2684
81 Wang Y, Liu W, Qu Z, Tan H, Liu Y, Xie G, Zhu W. *Dyes Pigments*, 2017, 143: 173–182
82 Nie H, Chen B, Zeng J, Xiong Y, Zhao Z, Tang BZ. *J Mater Chem C*, 2018, 6: 3690–3698
83 Wang H, Liu G, Dong S, Xiong J, Du Z, Cheng X. *J Mater Chem B*, 2015, 3: 7401–7407
84 Yan L, Zhang Y, Xu B, Tian W. *Nanoscale*, 2016, 8: 2471–2487
85 Li D, Qin W, Xu B, Qian J, Tang BZ. *Adv Mater*, 2017, 29: 1703643
86 Qian J, Tang BZ. *Chem*, 2017, 3: 56–91
87 Zhou Y, Hua J, Tang BZ, Tang Y. *Sci China Chem*, 2019, 62: 1312–1332
88 Gogoi A, Mukherjee S, Ramesh A, Das G. *Anal Chem*, 2015, 87: 6974–6979
89 Hu J, Liu R, Zhai S, Wu Y, Zhang H, Cheng H, Zhu H. *J Mater Chem C*, 2017, 5: 11781–11789
90 Horak E, Hranjec M, Vianello R, Steinberg IM. *Dyes Pigments*, 2017, 142: 108–115
91 Pan S, Liu W, Tang J, Yang Y, Feng H, Qian Z, Zhou J. *J Mater Chem B*, 2018, 6: 3927–3933
92 Jiang Y, Li G, Che W, Liu Y, Xu B, Shan G, Zhu D, Su Z, Bryce MR. *Chem Commun*, 2017, 53: 3022–3025
93 Zhao Z, Gao S, Zheng X, Zhang P, Wu W, Kwok RTK, Xiong Y, Leung NLC, Chen Y, Gao X, Lam JWY, Tang BZ. *Adv Funct Mater*, 2018, 28: 1705609
94 Liu D, Li J, Liu J, Lu X, Hu M, Li Y, Shu Z, Ni Z, Ding S, Jiang L, Zhen Y, Zhang X, Dong H, Hu W. *J Mater Chem C*, 2018, 6: 3856–3860
95 Zhu M, Yang C. *Chem Soc Rev*, 2013, 42: 4963–4976
96 Im Y, Byun SY, Kim JH, Lee DR, Oh CS, Yook KS, Lee JY. *Adv Funct Mater*, 2017, 27: 1603007
97 Cai X, Su SJ. *Adv Funct Mater*, 2018, 28: 1802558
98 Lee JH, Chen CH, Lee PH, Lin HY, Leung M, Chiu TL, Lin CF. *J Mater Chem C*, 2019, 7: 5874–5888
99 Park H, Lee J, Kang I, Chu HY, Lee JI, Kwon SK, Kim YH. *J Mater Chem*, 2012, 22: 2695–2700
100 Chercka D, Yoo SJ, Baumgarten M, Kim JJ, Müllen K. *J Mater Chem C*, 2014, 2: 9083–9086
101 Sun W, Zhou N, Xiao Y, Wang S, Li X. *Chem Asian J*, 2017, 12: 3069–3076
102 Tang X, Bai Q, Shan T, Li J, Gao Y, Liu F, Liu H, Peng Q, Yang B, Li F, Lu P. *Adv Funct Mater*, 2018, 28: 1705813
103 Shellaiah M, Wu YH, Singh A, Ramakrishnam Raju MV, Lin HC. *J Mater Chem A*, 2013, 1: 1310–1318
104 Wang C, Li L, Zhan X, Ruan Z, Xie Y, Hu Q, Ye S, Li Q, Li Z. *Sci Bull*, 2016, 61: 1746–1755
105 Feng X, Xu Z, Hu Z, Qi C, Luo D, Zhao X, Mu Z, Redshaw C, Lam JWY, Ma D, Tang BZ. *J Mater Chem C*, 2019, 7: 2283–2290
106 Zhang H, Li A, Li G, Li B, Wang Z, Xu S, Xu W, Tang BZ. *Adv Opt Mater*, 2020, 8: 1902195
107 Wang H, Li Y, Zhang Y, Mei J, Su J. *Chem Commun*, 2019, 55: 1879–1882
108 Wang H, Gu X, Hu R, Lam JWY, Zhang D, Tang BZ. *Chem Sci*, 2016, 7: 5692–5698
109 Wang Y, Lv MZ, Song N, Liu ZJ, Wang C, Yang YW. *Macromolecules*, 2017, 50: 5759–5766
110 Li X, Li Z, Yang YW. *Adv Mater*, 2018, 30: 1800177
111 Zhang JC, Pan C, Zhu YF, Zhao LZ, He HW, Liu X, Qiu J. *Adv Mater*, 2018, 30: 1804644
112 Bian L, Shi H, Wang X, Ling K, Ma H, Li M, Cheng Z, Ma C, Cai S, Wu Q, Gan N, Xu X, An Z, Huang W. *J Am Chem Soc*, 2018, 140: 10734–10739
113 Tao Y, Chen R, Li H, Yuan J, Wan Y, Jiang H, Chen C, Si Y, Zheng C, Yang B, Xing G, Huang W. *Adv Mater*, 2018, 30: 1803856
114 Zhang J, Tian H. *Adv Opt Mater*, 2018, 6: 1701278
115 Wu NMW, Ng M, Yam VWW. *Nat Commun*, 2022, 13: 33
116 Wang S, Wang F, Li C, Li T, Cao D, Ma X. *Sci China Chem*, 2018, 61: 1301–1306
117 Zhao J, Chi Z, Yang Z, Mao Z, Zhang Y, Ubba E, Chi Z. *Mater Chem Front*, 2018, 2: 1595–1608
118 Yang Z, Chi Z, Mao Z, Zhang Y, Liu S, Zhao J, Aldred MP, Chi Z. *Mater Chem Front*, 2018, 2: 861–890
119 Pramanik S, Deol H, Bhalla V, Kumar M. *ACS Appl Mater Interfaces*, 2018, 10: 12112–12123
120 Roy B, Reddy MC, Hazra P. *Chem Sci*, 2018, 9: 3592–3606
121 Zhuang W, Xu Y, Li G, Hu J, Ma B, Yu T, Su X, Wang Y. *ACS Appl Mater Interfaces*, 2018, 10: 18489–18498
122 Mellerup SK, Wang S. *Chem Soc Rev*, 2019, 48: 3537–3549
123 Huang G, Jiang Y, Yang S, Li BS, Tang BZ. *Adv Funct Mater*, 2019, 29: 1900516
124 Zhang J, He B, Hu Y, Alam P, Zhang H, Lam JWY, Tang BZ. *Adv Mater*, 2021, 33: 2008071
125 Chen Z, Liu J, Chen Y, Zheng X, Liu H, Li H. *ACS Appl Mater Interfaces*, 2021, 13: 1353–1366
126 Yang Z, Chi Z, Yu T, Zhang X, Chen M, Xu B, Liu S, Zhang Y, Xu J. *J Mater Chem*, 2009, 19: 5541–5546
127 Ou D, Yu T, Yang Z, Luan T, Mao Z, Zhang Y, Liu S, Xu J, Chi Z, Bryce MR. *Chem Sci*, 2016, 7: 5302–5306
128 Wang L, Yu T, Xie Z, Chen X, Yang Z, Zhang Y, Aldred MP, Chi Z. *J Mater Chem C*, 2018, 6: 8832–8838
129 Luo M, Zhao J, Liu Y, Jiang L, Wang S, Chi Z. *Adv Opt Mater*, 2022, 10: 2201195
130 Li N, Gu Y, Chen Y, Zhang L, Zeng Q, Geng T, Wu L, Jiang L, Xiao G, Wang K, Zou B. *J Phys Chem C*, 2019, 123: 6763–6767
131 Wang C, Yu Y, Yuan Y, Ren C, Liao Q, Wang J, Chai Z, Li Q, Li Z. *Matter*, 2020, 2: 181–193
132 Yu T, Ou D, Wang L, Zheng S, Yang Z, Zhang Y, Chi Z, Liu S, Xu J, Aldred MP. *Mater Chem Front*, 2017, 1: 1900–1904
133 Jiang S, Liu S, Meng L, Qi Q, Wang L, Xu B, Liu J, Tian W. *Sci China Chem*, 2020, 63: 497–503
134 Tao T, Gan Y, Zhao Y, Yu J, Huang Q, Yang Z, Chen M, Huang W. *J Mater Chem C*, 2019, 7: 3765–3771
135 Kong TT, Zhao Z, Li Y, Wu F, Jin T, Tang BZ. *J Mater Chem B*, 2018, 6: 5986–5991
136 Yan M, Feng S, Yu L, Xue Y, Huang J, Yang X. *Biosens Bioelectron*, 2021, 192: 113532
137 Yao H, Dai J, Zhuang Z, Yao J, Wu Z, Wang S, Xia F, Zhou J, Lou X, Zhao Z. *Sci China Chem*, 2020, 63: 1815–1824
138 Wang S, Chen C, Wu J, Zhang J, Lam JWY, Wang H, Chen L, Tang BZ. *Sci China Chem*, 2022, 65: 870–876
139 Li Y, Zhao Z, Zhang J, Kwok RTK, Xie S, Tang R, Jia Y, Yang J, Wang L, Lam JWY, Zheng W, Jiang X, Tang BZ. *Adv Funct Mater*, 2018, 28: 1804632